ANALYSIS AND MODELING OF BOILING FLUID SOLAR COLLECTORS

by

HENRY WALES PRICE

A thesis submitted in partial fulfillment of the
requirements for the degree of

MASTER OF SCIENCE
(Engineering)

at the

UNIVERSITY OF WISCONSIN-MADISON

1984

ACKNOWLEDGEMENTS

I Would like to thank Professor Sandford A. Klein for his help and interest in this research. How you find time for it all I'll never know. I would also like to thank Professor William A. Beckman for his forthright approach and Professor John A. Duffie for his answers to my many questions.

I also owe a debt of gratitude to the rest of the Solar Lab "Clan." A better group of people to work and associate with one could not hope to find. Thanks for your friendship and technical insight. Good luck all of you.

And finally to Denise for being there and putting up with me, and Ashley for helping me get an early start.

Financial support for this work has been provided by the Solar Heating and Cooling Research and Development Branch Office of Conservation and Solar Applications, U.S. Department of Energy.

Abstract

A boiling fluid (ie. R-11) can be used in place of air or non-boiling liquids as the heat exchange fluid. Claimed advantages for boiling fluid solar collectors (BFSCs) are increased heat transfer coefficients, inherent freeze protection, reduced parasitic energy use and improved transient response to changing meteorological variables. Several studies have been done and a separate test procedure for BFSCs has been developed. Still much confusion exists as to how these collectors work and how they can be modeled, and whether or not the new testing procedure is necessary. This research attempts to clear up some of the questions about BFSCs. Two models were developed for use with TRNSYS to analyze BFSCs. One is an ideal model which models BFSCs as standard collectors with a condenser for a heat exchanger. The second more detailed (non-ideal) model is capable of modeling a wide range of BFSC types and operating conditions.

The boiling collector used in this study is representative of one currently in the marketplace for domestic water heating. The system uses a flat-plate solar collector and an external coiled heat exchanger for a condenser. The performance of the boiling collector itself

is not as much interest as the performance of the boiling collector-condenser combination. The models developed here consider the collector and condenser together as a single TRNSYS component.

The ideal model involves a modification to the collector heat removal factor, F_R, to account for the effect of the condenser. It is assumed that saturated liquid enters the collector and saturated vapor exits. Pressure losses in the connecting lines are neglected. With these assumptions, the efficiency of the collector-condenser combination is shown to be a linear function of $(T_i - T_a)/I$, where T_i is the condenser water inlet temperature, T_a is the ambient air temperature, and I is the solar flux incident upon the collector. The efficiency curve has the same form as that of conventional (ie, non-boiling) flat-plate collectors. As a result, the f-Chart method can be used to predict the long-term performance of boiling collector systems. The assumptions made in this model are optimistic and yield a maximum performance estimate. However, studies done with the detailed model show that the sensitivity of long-term performance to sub-cooling and moderate pressure losses is small.

The first non-ideal model allows a detailed analysis of the boiling collector. This model can account for a

subcooled liquid entering the collector, dryout and superheating in the collector, heat losses in the vapor and the liquid return line, pressure drops due to friction in the collector and piping, and pressure drops due to the hydrostatic head of the fluid. The model has been used to determine the yearly performance of boiling flat-plate solar collectors.

Parametric studies were performed to determine the relative sensitivity of yearly performance for many parameters in the model. The effects of diameter and length of the refrigerant pipes on system performance was determined. Other effects such as changing refrigerants, collector area, condenser size, and geographic location were also studied. Temperature stratification in the storage tank has been shown to improve collector performance (Wuestling). This is usually accomplished by reducing the mass flow rate of water through the collector. In the case of a boiling collector, the mass flow rate of water through the condenser must be reduced. The optimum condenser water mass flow rates were determined for several locations.

TABLE OF CONTENTS

LIST OF FIGURES

LIST OF TABLES

NOMENCLATURE

A	surface area
C_{bond}	collector plate to riser resistance
C_o	two-phase flow parameter (ref 25)
C_p	specific heat
D	outside diameter
d	inside diameter
f	friction factor
F	collector fin efficiency
F'	collector efficiency factor
F''	collector flow factor
F_R	collector heat removal factor
F'_R	collector heat exchanger factor
F_{boil}	boiling collector heat removal factor
g	gravitational constant
G	mass flux
G_T	irradiance on tilted surface
h	heat transfer coefficient
i	enthalpy
j	volumetric flux
L	length in flow direction
$\dot{m}$	mass flow rate
NTU	number of transfer units

P	pressure
Q	energy per unit time
Re_D	Reynolds Number
S	absorbed solar radiation per unit area
T	temperature
UA	heat transfer conductance
u_{gj}	drift velocity
U_L	collector loss coefficient
v	velocity
W	distance between collector riser tubes
X	quality
Z	axis in direction of flow in collector
α	absorptance
β	collector slope of volumetric quality
ε	heat exchanger effectiveness
η	collector efficiency
μ	viscosity
ν	specific volume
ρ	density
τ	transmittance
ϕ	friction multiplier
κ	fin effectiveness

Subscripts

b	boiling or boiling section of collector
bp	boiling point elevation
c	collector or cold
cond	condenser
d	dryout portion of collector
f	fluid or liquid
h	hot
i	inlet
l	liquid
loss	heat losses
LMTD	log mean temperature difference
o	outlet
rl	liquid return line
sat	saturation
sc	subcooled
sh	superheated
TP	two-phase
u	useful
v	vapor
vl	vapor line
W	water

1. INTRODUCTION

The purpose of a solar collector is to transform solar radiant energy into a more useful form of energy. Typically the desired result is the conversion to thermal energy for water or space heating purposes. A working fluid such as water or an antifreeze solution is generally used to transfer the thermal energy from the collector to a heat-exchanger or storage tank. The working fluid is heated as it passes through the collector. An alternative which has been recieving more attention in recent years is to use a boiling or phase-change working fluid in the collector as the heat-transfer medium. When energy is transferred from the collector to the fluid, the fluid changes phase from a liquid to a vapor.

Several studies have been done with boiling fluid solar collectors. A separate test procedure has been developed for boiling fluid flat-plate solar collectors (ASHRAE 109). Still much confusion exists as to how these collectors work, how they can be modeled, and whether or not the new testing procedure is necessary. This research is an attempt to clear up some of the questions about boiling fluid solar collectors. It specifically it deals

with the analysis of boiling fluid solar collector systems, and the development of an analytical model which can be used to study the performance of boiling fluid solar collectors. This chapter presents an introduction to boiling fluid solar collectors, a description of a boiling fluid collector systems and their operation, a literature review, a description of the simulation program used in this study, a discussion of important thermodynamic and transport properties of boiling fluids, and the objectives of this study.

1.1 Boiling Fluid Solar Collectors

A boiling fluid (e.g. an organic refrigerant) can be used in place of air or non-boiling liquids as the heat exchange fluid in a solar collector.

The configuration of a boiling fluid solar collector (BFSC) system is similar to a standard hydronic collector system which utilizes an antifreeze loop with a heat exchanger for freeze protection. In the standard system an anti-freeze solution is circulated by pump in the primary heat exchange loop between the collector and a heat-exchanger. Water would be circulated by pump through the secondary heat exchange loop between the heat-exchanger and a storage tank. The BFSC system is identical to the hydronic system, except that the fluid in the primary loop

boils as it passes through the collector and condenses in the heat-exchanger. The circulation of refrigerant in the primary heat exchange loop can be by pump but is most commonly caused by the thermosyphoning action provided by the boiling and condensing of the refrigerant.

Boiling fluid solar collectors can be grouped into two general categories depending on where the condenser is located. The first type has its condenser located inside the collector box. Thus the boiling and the condensing occurs within the collector. This has the advantage that the collector can be pre-charged at the factory, which simplifies installation. Freeze protection in the water loop is provided by circulating hot water from the storage tank through the condenser. Losses from the collector are minimal due to the diode effect of the boiling fluid. The second type of BFSC has its condenser located external to the collector. The collector and condenser are connected by two pipes, a vapor supply line and a liquid return line. For this type of system it is usually necessary to have a refrigeration or air conditioning specialist install and charge the system, since they are usually assembled on site. Freeze protection for this type of BFSC can be provided by locating the condenser in a heated space. The analysis of these two types of systems is identical. The

second type is a more generalized system and is used for developing a model.

Claimed advantages for using an organic refrigerant in BFSCs are: inherent freeze protection, prevention of fouling and corrosion in the collector, pipes and heat exchanger, low maintance, easy leak detection during installation, increased heat transfer coefficients in collector and heat exchanger, reduced plate losses, improved transient response, and reduced parasitic energy requirements. If non-organic refrigerants are used some of these advantages may not exist. Water, for example, could be used as the boiling fluid or refrigerant but it does not provide freeze protection.

Several disadvantages exist for BFSCs: boiling collector systems tend to be more expensive than standard hydronic or air collector systems, installation may require refrigerant specialists, thermosyphon systems require the condenser to be located above the collector, the condenser must have some form of freeze protection or be located in a heated space and leaks of organic refrigerants to the environment are undesirable.

1.2 System Description and Operation

To aid in the analysis and modeling of BFSCs, a specific system configuration was chosen to be studied. Figure 1.2.1 is a schematic of a boiling fluid solar collector system with an external condenser. It is a 2 tank solar domestic hot water (SDHW) system. The boiling collector and condenser used in this study are representative of products in the market place for domestic space and water heating. The system uses a flat-plate collector and a coiled heat exchanger for a condenser. The primary heat exchange fluid operates in a thermosyphon mode. Water is circulated through the secondary loop between the condenser and the preheat tank. An auxiliary tank with heating elements is included to ensure that the water is supplied at the set temperature. When a load is drawn from the tank, solar heated water from the preheat tank replaces it. A tempering valve is included which limits the temperature of the delivered water, if necessary, by mixing it with mains water to achieve the set temperature. Figure 1.2.2 is a diagram of the primary heat exchange loop which contains the boiling fluid. Initially the collector loop is only partially filled with refrigerant, enough to fill the collector 2/3 to 7/8 full of liquid. The liquid cannot circulate by itself. When

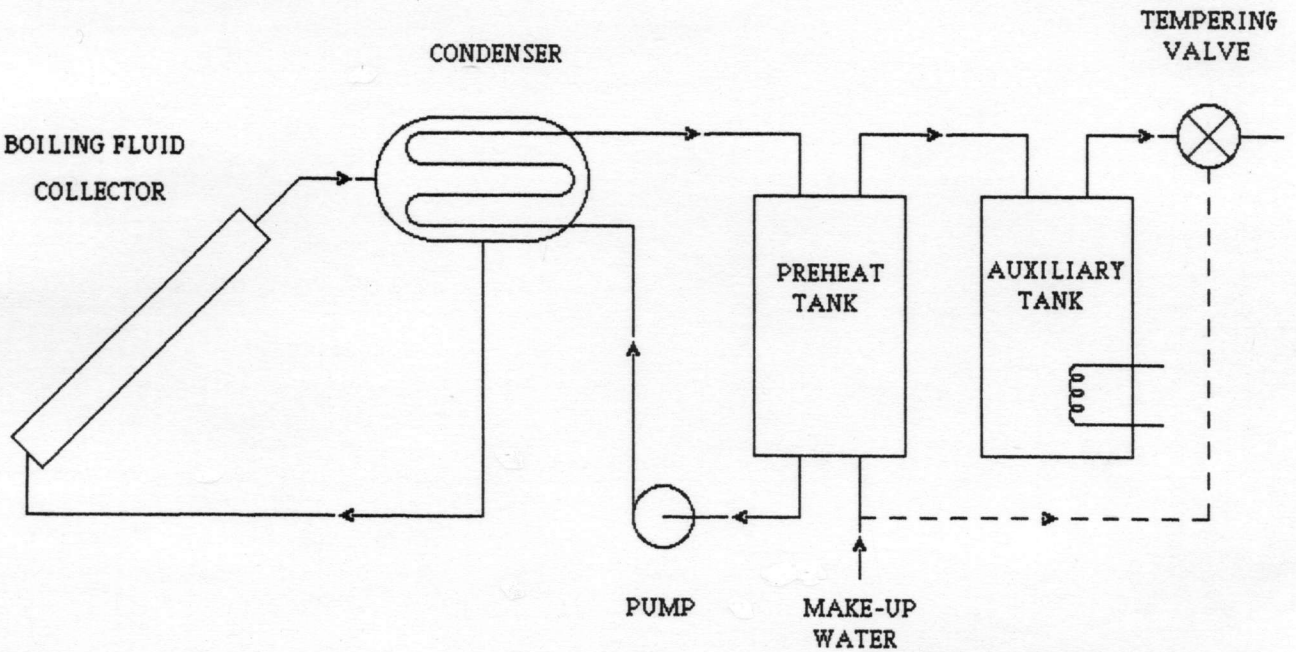

FIGURE 1.2.1 Boiling Fluid Solar Collector System

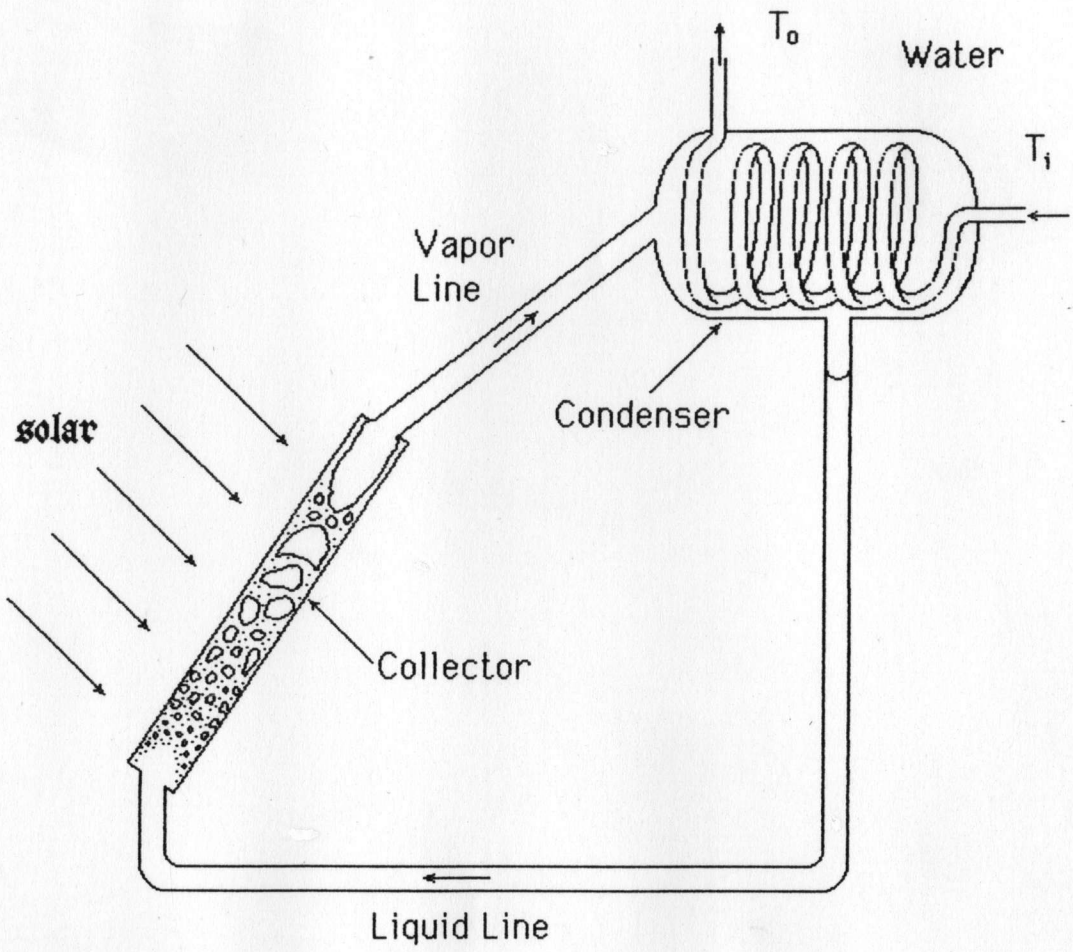

Figure 1.2.2 Boiling Fluid Solar Collector

the absorbed solar radiation is sufficient to overcome collector losses to the environment, the liquid refrigerant is heated and begins to boil. At this point the fluid becomes a two phase mixture as the liquid vaporizes. The average density of the fluid is reduced as vapor forms causing the vapor and entained liquid to rise in the collector. At the top of the collector a separator separates the vapor and liquid. The liquid is refluxed to the bottom of the collector and the vapor continues to rise through the vapor line to the condenser. When the temperature in the condenser reaches a specified temperature above the water temperature in the bottom of the preheat tank, the circulation pump in the secondary loop is activated. The vapor is condensed by heat transfer to the circulating water, drips off, and returns down the liquid return line. The thermosyphon action will continue as long as the condenser is below the saturation temperature of the entering vapor.

1.3 Literature Review

Literature relating to boiling fluid solar collectors can be broken into several areas: general information, experimental testing, analytical modeling and test procedures. The first area, general information covers papers dealing with the general topic of boiling fluid

solar collectors. According to McLaughlin of SRCC (1), there is and urgent need for additional fundamental research on the topic of BFSCs. The ASHRAE Standard 93-77 (2) cannot be used to test these kinds of collectors, since they rely on a phase-change heat transfer fluid in the collector. A new ASHRAE Standard 109 (3) has been introduced but the Hottel-Whillier collector efficiency equation does not apply. Thus the f-Chart method cannot be used to determine yearly performance of systems with BFSCs. Some collectors show sensitivity to solar irradiation levels. It is necessary to develop a testing method for BFSCs which accounts for this and can be used to help determine the long term performance. Best (4) discusses the advantages of boiling fluid or phase change solar collectors containing organic refrigerants. He also looks into the problem of ozone leaks into the atmosphere. Sands (5) presents 15 different phase-change collector systems which are currently on the market place. The systems are broken into 4 groups: passive, partly passive, active and high temperature systems. Passive systems generally have the condenser located in the tank. Partly passive systems rely on thermosyphoning of the phase-change liquid like the passive systems but pump water through the condenser. Active systems simply use the refrigerant as the heat

exchange fluid, and the fluid may or may not boil. The high temperature systems are evacuated tubular heat pipes. All the systems utilize flat-plate collectors except the high temperature systems.

Several studies have been completed which experimentally test different boiling fluid collector systems. Evans and Greeley (6) and Rush (7) have developed and tested thermosyphoning flat-plate boiling fluid solar collectors and found that they had many advantages over standard hydronic systems. Soin et al (8) studied a boiling thermosyphon collector containing acetone and petroleum ether mixture and developed a modified form of the Hottel-Whillier equation (9) which would account for the fraction of liquid level in the collector. Schreyer (10) experimentally investigated the use of a thermosyphon refrigerant (R-11) charged solar collector for residential applications. He found that for two identical collectors a boiling refrigerant charged collector out performed a hydronic fluid circulating solar collector. Downing and Waldin (11) studied the heat transfer processes in boiling solar domestic hot water (SDHW) systems using R-11 and R-114. They determined that phase change heat transfer fluids operate with better efficiency and faster response than circulating liquids in solar applications. Fanney and

Terlizzi (12) used the ASHRAE Standard 93-77 test procedure (2) to determine the thermal performance of a boiling fluid flat-plate collector-condenser system. They found that the collector-condenser system did not exhibit a dependence on solar radiation.

The Solar Energy Applications Laboratory at Colorado State University (13) has studied the long term performance of evacuated tubular heat pipe solar collectors. The heat pipe collectors were used for both heating and cooling of their Solar House 1. The study concluded that the heat pipe collector has a high operating efficiency even while delivering water temperatures above 120 C. An empirical expression was developed for the heat pipe collector efficiency. Three other parameters were required: $(T_i - T_a)^2/G_T$, $(T_i - T_a)$ and G_T, were required in addition to the traditional $(T_i - T_a)/G_T$ parameter from the Hottel-Whillier equation to adequately represent the efficiency of heat pipe collectors.

Two detailed analytical studies of boiling fluid solar collectors have been completed. The first was done by Al-Tamimi (14) and by Al-Tamimi and Clark (15,16). They tested a boiling collector and developed an analytical model to investigate the effect on collector efficiency of subcooling the fluid entering the collector, and the level

of fluid in the collector. They also investigated the fluid circulation rate, the system pressure drop, the temperature distribution in the collector, stagnation conditions, and the collector dynamic response. One of the primary results of this work was that collector efficiency was found to be a strong function of solar radiation, as shown in figure 1.3.1, unlike non-boiling collectors which show almost no solar radiation dependence. If the fluid entering the collector is below its boiling temperature at the pressure it enters the collector, it must be heated up before it will begin to boil. Z^* is defined as the fraction of the collector required to heat the fluid to its boiling temperature. Figure 1.3.1 shows lines of constant Z^*. A second important result was that the flow rate of refrigerant through the collector was a linear function of the intensity of solar radiation. The function, however, would be unique for each collector installation depending on the system configuration. A modification of the collector heat removal factor, F_R, in the Hottel-Whillier collector equation was developed to account for the boiling and the subcooled portions of the flat-plate boiling collector. However to use this equation, Z^* and the mass flow rate of refrigerant through the collector must be known. Variations in the thermodynamic properties of R-11

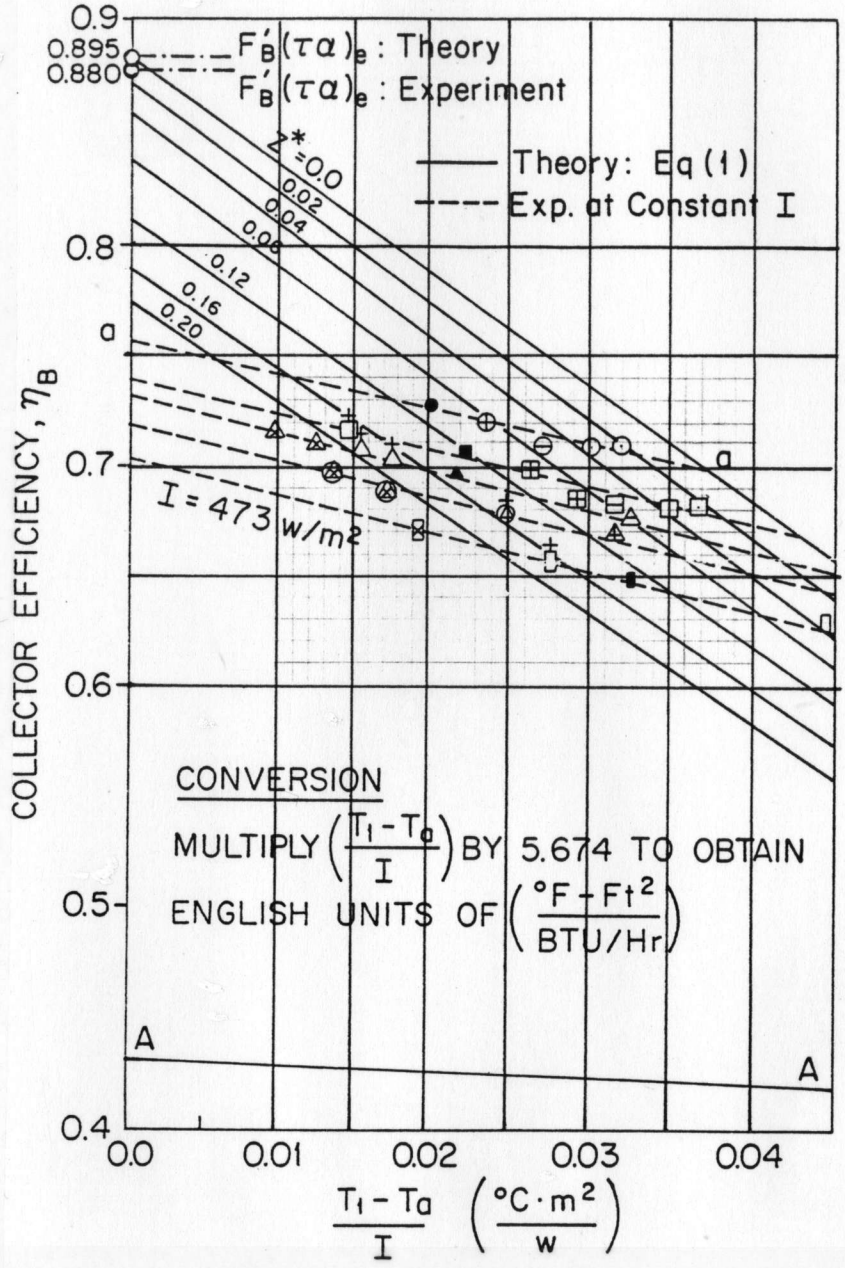

1.3.1 Thermal Efficiency of a Boiling Fluid Solar Collector [Taken from ref. (5)]

were not considered in this study.

The second analytical study was completed by Abramzon, Yaron and Borde (17). They developed a mathematical model for the efficiency of a flat-plate collector containing a boiling fluid. They found that the efficiency of a flat-plate collector with internal boiling approaches the ideal collector efficiency. The ideal collector efficiency occurs when the internal fluid heat transfer coefficient is infinite. The type of boiling fluid used did not make any appreciable difference in the collector performance for cases with little subcooling. The reduction in collector efficiency caused by subcooling of 5 to 10 C in the collector was negligable due to the high heat transfer associated with subcooled boiling. One important result was that the collector efficiency was dependent on the level of solar radiation incident on the collector. No explanation was given as to the reason for this occurrence.

A recent ASHRAE Standard (109) was developed for testing the thermal performance of flat-plate solar collectors containing a boiling liquid (3). The testing procedure is based largely upon the analytical methods developed by Al-Tamimi and Clark (16). The test is similar to the 93-77 test except that 3 separate tests of instantaneous thermal efficiency at different levels of

subcooling are required: no subcooling ($\Delta T_{sc} < 3$ C), and subcooled entering states of 6 and 15°C. These tests are designed to determine the dependence of efficiency on the intensity of solar radiation, and the effect of subcooling on efficiency. The 109 Standard also requires the determination of the collector time constant.

1.4 TRNSYS

The BFSC water heating system in Figure 1.2.1 was modeled using the TRNSYS 12.1 (18). TRNSYS is a modular transient system simulation program, which is used for detailed analysis of systems whose behavior is dependent on time. The modular nature gives the program flexibility to be used in many thermodynamic processes, and enables the user to develop components (mathematical models) not in the standard TRNSYS library. Components are typically mathematical models of the systems used in an actual solar heating system. Typical components are solar collectors, pumps, tanks, controllers, loads, etc,. Other components model physical processes such as the solar radiation processor, and finally other components are used to input or output data. The Boiling collector-condenser system model in this study employed standard TRNSYS library components for the tanks, the pump, controls, and solar

radiation processing. The system incorporates a daily mass flow load profile developed by a Rand Corporation Survey (19) for a "typical" residence.

Since the condenser is an integral part of the boiling collector-condenser system a single component was developed to model the boiling collector and condenser.

1.5 Refrigerant Properties

There is an almost endless list of refrigerants which could be used in a boiling fluid solar collector. Refrigerants R-11, R-12, R-22, R-113, R-114, R-717 (ammonia), and R-718 (water), are some if the common refrigerants used in heating and cooling applications today. In order to determine which refrigerant should be used in a boiling fluid solar collector, it is useful to see how different thermodynamic, transport and other properties of refrigerants effect the performance and physical design of the boiling fluid collector system. In this section the following properties are considered: vapor pressure, latent heat of vaporization, specific heat of the liquid, liquid density, decomposition rate of refrigerants, freezing point, and the critical temperature.

The vapor pressure of the refrigerant determines the working pressure in the primary heat exchange loop. The collector, piping and condenser must be designed to withstand the pressures developed by the refrigerant at stagnation temperatures. For refrigerants with high vapor pressures this means added material costs. R-12 and ammonia are examples of refrigerants which have high vapor pressures. The saturation boiling temperatures of refrigerants with high vapor pressures, tend to be less sensitive to frictional and hydrostatic pressure drops in the collector loop. In general vapor pressures of refrigerants tend to be higher than that of water.

The mass flow rate of fluid around the collector loop in boiling fluid solar collectors is an order of magnitude less than the mass flow rates used in typical hydronic collectors. This difference is due to the large amount of energy which can be stored in the form of latent heat as compared with the much smaller specific heat of the fluid. A high latent heat of vaporization is desired in a boiling fluid collector system. Most of the energy transferred is by the latent energy stored in the vapor. The flow rate of refrigerant can be reduced by using a fluid with a high latent heat of vaporization. The advantage is that smaller pipes can be used. The heat of vaporization of most

refrigerants is approximately an order of magnitude less than that of water.

The specific heats of most organic refrigerants are only about 25% of that of water. This improves the response time of the collector and may reduce heat losses from the piping. The main disadvantage of fluids with low specific heats is that they reduce the thermal performance of the subcooled portion of the collector.

The liquid density of most organic refrigerants is about 1.5 times that of water. Pumps, if used, must account for this. The expansion of refrigerants is also much greater than water at the temperatures considered.

Most organic refrigerants are known to break down at high temperatures. R-11 for example, decomposes at a rate of 1%/year at 282 C. In the temperature ranges used in most domestic solar applications, the decomposition is negligable. It generally is not necessary to change the working fluid over the lifetime of the collector.

The freezing point of a refrigerant is another important property. The primary disadvantage to using water as the refrigerant is that it freezes at 0 C. Organic refrigerants on the other hand freeze at temperatures much lower.

The critical temperature of the refrigerant can be used as a temperature limiting device, to reduce high stagnation temperatures which can occure. This is often used in evacuated tube heat pipe systems where temperatures well in excess of 100 C are easily obtained. In these systems when the critical temperature is reached the fluid can no longer condense, so heat transfer to the condenser is limited to free convection of the gas in the collector.

The most common refrigerants used in boiling fluid solar applications are: R-11, R-12, R-113, and R-114.

1.6 Objective

Even with all the work which has been completed, much confusion exists as to how these these boiling fluid collectors work, how they can be modeled, and whether or not they require a separate new testing procedure. This thesis will attempt to clear up some of these questions and provide a general study on boiling (2-phase) solar collectors. Chapter 1 has been a introduction to boiling fluid solar collectors, describing the collectors and their operation, a review of the literature and a description of refrigerants and important considerations when choosing one.

Chapter 2 looks at an ideal boiling fluid solar collector. The assumptions of the ideal collector are listed. A model to calculate the useful energy gain of an ideal boiling fluid collector is developed. The results of the ideal model are compared with experimental data.

Chapter 3 studies the non-ideal boiling collector. The effect on performance and the causes of subcooling, dryout, superheating, pressure drops and heat losses are considered. An analitical model for calculating collector efficiency is developed which accounts for each of the above topics. Several models of boiling fluid flow are evaluated for modeling two-phase flow in a solar collector.

Chapter 4 applies the models developed in the previous chapters. Parametric studies are performed to determine the effect on annual collector performance of refrigerant type, collector area, condenser area and optimum condenser water mass flow rate. A comparison is made between the ideal and the non-ideal models. A second comparison is made between hydronic and boiling fluid solar collectors.

Chapter 5 analyzes the boiling section of the collector in more detail than chapter 3. Several models of boiling fluid flow are evaluated for modeling two-phase flow in a boiling fluid solar collector.

Chapter 6 draws conclusions from the results presented in previous chapters as to the application and usefulness and the most appropriate methods of testing boiling fluid solar collectors. Recommendations for further study are included.

2. Ideal Boiling Fluid Solar Collector

In this chapter an analytical model is developed to study the performance of an ideal boiling fluid solar collector (BFSC). The ideal BFSC concept is a useful form of first analysis, and it is a fairly simplified approach which gives an upper bound on the obtainable performance. This chapter looks at the following topics: the assumptions required for the ideal boiling fluid solar collector, the development of an analytical model for determining instantaneous collector efficiency, and the results of the model are compared with experimental data.

2.1 Assumptions

Several assumptions are necessary for the ideal BFSC. The first assumption is that the fluid (refrigerant) enters the collector as a saturated liquid. Any energy gained by the collector will immediately cause the fluid to boil. A second assumption is that the fluid leaves the collector as a saturated vapor. Thus there is no entrainment of liquid in the vapor, and no superheating of the vapor before it exits the collector. Boiling heat transfer occurs the entire length of the collector. Third, at any given time the boiling processes in the collector and condenser occur at a constant pressure. Thus the temperature will be

constant along the length of the collector, and the temperature in the condenser is the same as the temperature in the collector. Fourth, the boiling heat transfer coefficient is assumed to be constant and will not vary as the quality of the refrigerant changes. This implies that the collector plate temperature will also be independent of distance in the flow direction. Fifth, all the energy gained in the collector is assumed to be removed at the condenser. Thus no energy is dissipated as friction, and there are no thermal losses except in the collector itself. Finally, the heat transfer coefficients in the collector (h_{fi}) and condenser (UA_{cond}) are assumed to be constant, and do not vary under different operating conditions. However, in a BFSC not only the temperature varies with changing meteorological variables, but also the mass flow rate of refrigerant varies. Thus, the assumptions that h_{fi} and UA_{cond} remain constant are not as good as they might be in a standard hydronic collector.

2.2 Analytical Model

The topic of interest when evaluating a BFSC, is not the efficiency of the collector, but the over all efficiency of the collector-condenser combination. The model developed here combines the collector and condenser into a single component. The basic structure of the ideal boiling collector-condenser model is an energy balance

which assumes a quasi-equilibrium state such that the energy gain of the collector equals the energy transfer to the water in the condenser. The ideal model assumes that the entire collector is in a fully boiling condition and at a constant temperature, (i.e. no subcooling, superheating, pressure drops, heat losses or property variations), and thus:

$$Q_u = Q_{cond} \tag{2.2.1}$$

Heat transfer in the condenser is modeled using a log-mean temperature difference with a heat transfer coefficient in the condenser of UA_{cond}.

$$Q_{cond} = UA_{cond}\ \Delta T_{LMTD}$$

$$Q_{cond} = \frac{UA_{cond}\left[(T_{sat} - T_o) - (T_{sat} - T_i)\right]}{\ell n\left[\frac{T_{sat} - T_o}{T_{sat} - T_i}\right]} \tag{2.2.2}$$

Where T_{sat} is the saturated boiling temperature in the collector and condenser, T_i is the temperature of the water entering the condenser, and T_o is the temperature of the water leaving the condenser. The heat transfer in the condenser can also be written:

$$Q_{cond} = (\dot{m}\ C_p)_W (T_o - T_i) \tag{2.2.3}$$

Where $(\dot{m}\ C_p)_W$ is the mass capacitance rate of the water in

the condenser. The collector-condenser model assumes that only condensation heat transfer occures in the condenser, and no subcooling of the condensed liquid. This is a good assumption for fluorocarbon refrigerants in a drip style condenser.

The heat transfer in a boiling flat-plate collector can be modeled in a similar manner as a flat-plate hydronic collector, with the assumption that the fluid boils at a constant pressure, and thus a constant temperature. The basic Hottle-Whillier collector equation for a boiling flat-plate collector (16) is:

$$Q_u = A_c F_R\{S - U_L (T_{sat} - T_a)\} \tag{2.2.4}$$

Where:

$$S = (\tau\alpha) G_T \tag{2.2.5}$$

$$F_R = F_{boil} \tag{2.2.6}$$

$$F_{boil} = \frac{1}{\frac{W U_L}{\pi D h_{fi}} + \frac{W U_L}{C_{bond}} + \frac{W}{D+(W-D) F}} \tag{2.2.7}$$

Where $(\tau\alpha)$ is the transmittance absorptance product, G_T is the instantaneous radiation on a tilted surface, and h_{fi} is the boiling heat transfer coefficient between the fluid and the collector riser tube.

Assuming that G_T, T_a, and T_i Are known, Q_u can be solved for using equations 2.2.1 - 2.2.8. Combining (2.2.2) and (2.2.3) and solving for T_o:

$$T_o = T_{sat} - (T_{sat} - T_i) \exp\left(\frac{UA_{cond}}{(\dot{m}\ C_p)_W}\right) \qquad (2.2.8)$$

Substituting this into equation (2.2.3) and solving for T_{sat}:

$$T_{sat} = \frac{Q_{cond}}{(\dot{m}\ C_p)_W \left[1 - \exp\left(\frac{UA_{cond}}{(\dot{m}\ C_p)_W}\right)\right]} + Ti \qquad (2.2.9)$$

Substituting for T_{sat} in (2.2.4) and assuming $Q_{cond} = Q_u$ and solving for Q_u, you get:

$$Q_u = \frac{A_c\ F_R\{S - U_L\ (T_i - T_a)\}}{1 + \frac{A_c\ F_R\ U_L}{(\dot{m}\ C_p)_W \left[1 - \exp\left(\frac{UA_{cond}}{(\dot{m}\ C_p)_W}\right)\right]}} \qquad (2.2.10)$$

Note that equation 2.2.10 can be directly solved for Q_u.

2.3 Modified Collector Heat Removal Factor

An alternative to the method used in the previous section to solve for the useful gain in the collector is to use a modified collector heat removal factor. The following F_R', was defined by deWinter (20) to account for the effect of a heat exchanger.

$$F_R' = \frac{F_R}{1 + \left[\frac{A_c F_R U_L}{(\dot{m} C_p)_c}\right]\left[\frac{(\dot{m} C_p)_c}{\varepsilon (\dot{m} C_p)_{min}} - 1\right]} \qquad (2.3.1)$$

ε, the effectiveness of the heat exchanger is:

$$\varepsilon = \frac{1 - \exp\{-NTU(1 - C^*)\}}{1 - C^* \exp\{-NTU(1 - C^*)\}} \qquad (2.3.2)$$

where:

$$NTU = \frac{(UA)_{cond}}{(\dot{m} C_p)_{min}} \qquad (2.3.3)$$

$$C^* = \frac{(\dot{m} C_p)_{min}}{(\dot{m} C_p)_{max}} \qquad (2.3.4)$$

Thus by knowing the effectiveness of the heat exchanger and the capacitance rates of the two streams, it is possible to determine the performance of a collector with a heat exchanger. The utilizable energy gain of the collector can then be written:

$$Q_u = A_c F_{R,boil}' \{S - U_L (T_{sat} - T_a)\} \qquad (2.3.5)$$

Where T_i is the temperature of the water entering the heat exchanger from the storage tank, and not the temperature of the fluid entering the collector.

For the case when the heat exchanger is a condenser, the above equations can be simplified since:

$$(\dot{m}\ C_p)_{max} \gg (\dot{m}\ C_p)_{min} \tag{2.3.6}$$

Thus:

$$C^* = 0 \tag{2.3.7}$$

$$NTU = \frac{(UA)_{cond}}{(\dot{m}\ C_p)_W} \tag{2.3.8}$$

The effectiveness of a condenser is then:

$$\varepsilon = \exp\left(\frac{-UA_{cond}}{(\dot{m}\ C_p)_W}\right) \tag{2.3.9}$$

The modified collector heat removal factor for a condenser can then be written:

$$F_{R,boil}' = \frac{F_R}{1 + \dfrac{A_c\ F_R\ U_L}{(\dot{m}\ C_p)_W \left[1 - \exp\left(\dfrac{UA_{cond}}{(\dot{m}\ C_p)_W}\right)\right]}} \tag{2.3.10}$$

If equation (2.3.10) is substituted into equation (2.3.5), the result is the same as equation (2.2.10). Both of these techniques take into account the effects of the condenser when calculating the useful energy gain in a boiling collector. Equation (2.3.10) can be rearranged to determine the penalty in collector performance caused by the added resistance to heat flow of the heat exchanger (condenser).

$$\frac{F_R'}{F_R} = \frac{1}{1 + \dfrac{A_c F_R U_L}{(\dot{m} C_p)_W \left[1 - \exp\left(\dfrac{UA_{cond}}{(\dot{m} C_p)_W}\right)\right]}} \qquad (2.3.11)$$

The efficiency of an ideal boiling fluid solar collector can be written:

$$\eta = F_R'(\tau\alpha) - \frac{F_R' U_L (T_i - T_a)}{G_T} \qquad (2.3.12)$$

Since F_R' is not a function of T_i, T_a or G_T, the plot of efficiency verses ΔT / G_T should be a straight line, similar to standard hydronic collectors. It is important to note again that T_i is the temperature of the water entering the condenser, and not the temperature of the refrigerant entering the collector.

2.4 Results

The ideal boiling fluid collector model developed in this chapter was used to analytically model the BFSC tested by Fanney (12). The parameters used in the model were the values experimentally determined by the National Bureau of Standards during the testing of the collector. The NBS collector was a two cover flat-plate thermosyphoning BFSC. Appendix A lists the collector dimensions and property values of the materials. Other values, such as condenser UA and $(\tau\alpha)$, were analytically determined using the

physical characteristics of the system. Figure 2.4.1 is a graph of collector efficiency verses $(T_i - T_a) / G_T$ and shows the results of the model as well as the actual test data obtained by Fanney. It is important to note the linearity of the experimental data. There does not appear to be any detectable solar radiation dependence in the data. In this case the boiling fluid solar collector model appears to be adequate. The reason the model somewhat under predicts the experimental data is likely due to an over prediction of the collector loss coefficient (U_L), or the under prediction of the boiling heat transfer coefficient in the collector (h_{fi}). Neither of these parameters are measured directly. Although the agreement between the model and the test data is remarkably good, the model may not be as close under other test conditions. For example, the NBS test used an ambient temperature of 20 C. If the ambient temperature had been much lower, heat losses from the refrigerant lines might have affected the instantaneous efficiency of the BFSC.

2.5 Summary

In this chapter, the concept of the ideal boiling fluid solar collector was introduced. It is in essence a solar collector which relies on boiling heat transfer throughout the entire collector, and which all the energy gained in the collector is retrieved at the condenser. Two

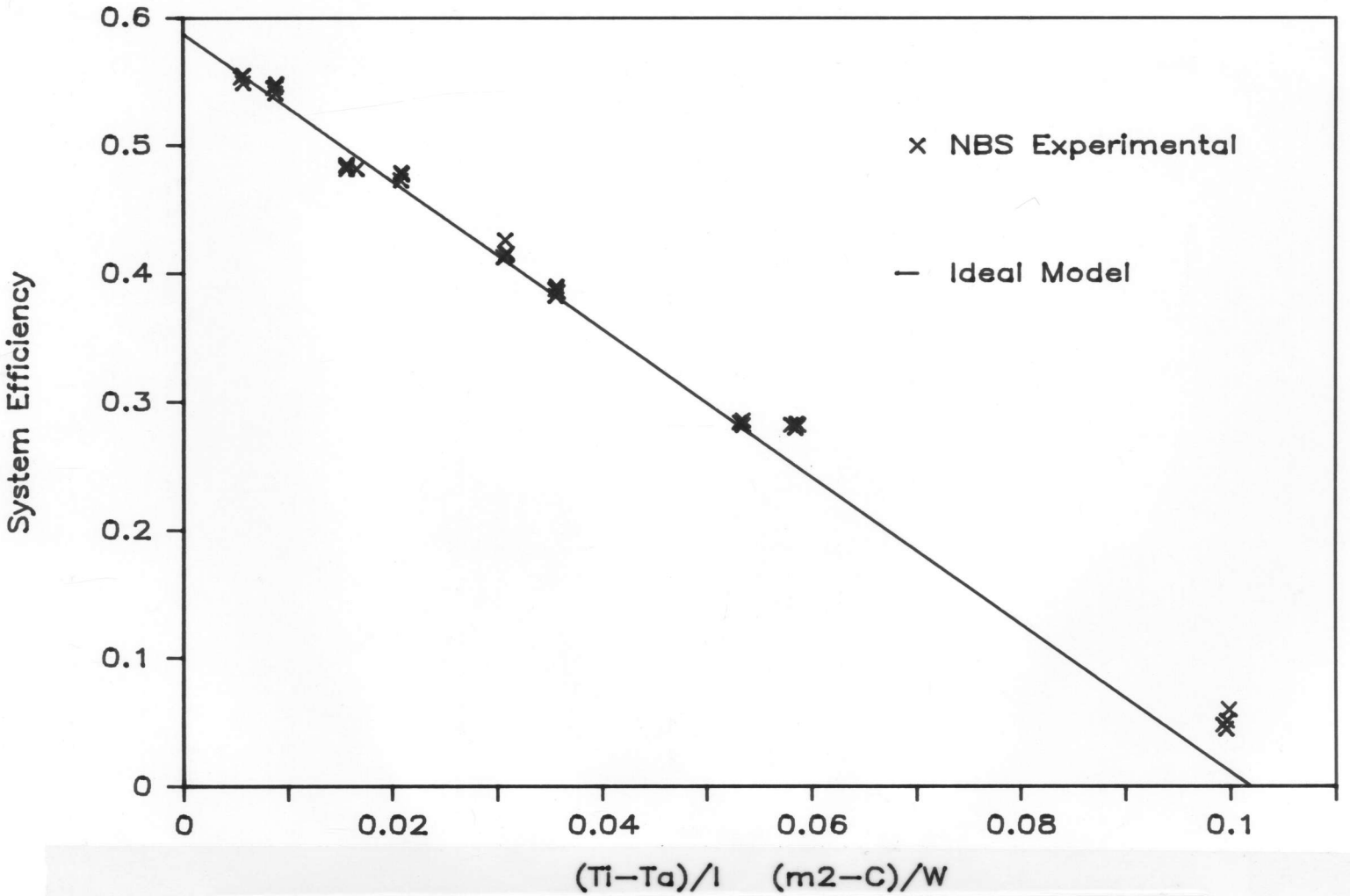

2.4.1 Instantaneous Thermal Efficiency of Ideal Boiling Fluid Solar Collector Model

approaches were taken for developing a model to determine the useful gain in the collector-condenser system. These were shown to give the same result. Finally the model was applied to a specific boiling fluid solar collector to determine its efficiency. This result was then compared with experimental data taken for this same collector. For the particular collector-condenser system studied, the ideal boiling fluid model does a good job predicting the instantaneous thermal performance.

The instantaneous efficiency curve for an ideal BFSC has the same form as that of conventional (ie, non-boiling) flat-plate collectors. As a result, the f-Chart method can be used to predict the long-term performance of ideal BFSC systems. The assumptions made in this model are optimistic and yield a maximum performance estimate.

3. Non-Ideal Boiling Fluid Solar Collector

The previous chapter dealt with an ideal boiling fluid solar collector. This chapter considers the non-ideal case of the boiling fluid solar collector (BFSC). Several assumptions were required for the ideal case which may not be reasonable for real BFSCs. In this chapter a more detailed model is developed which accounts for many of the situations which can occur in actual BFSCs. Subcooling, dryout, superheating, pressure variations, and heat losses are considered. The model is used to evaluate the effect on collector performance for each of these situations. But first, a generalized introduction to non-ideal boiling fluid collectors is given. This includes a discussion on the collector temperature profile and the general approach taken to model non-ideal boiling fluid collectors.

3.1 Introduction

The primary difference between the ideal and the non-ideal BFSCs, is that the ideal collector assumes that the entire collector exists in a 2-phase state and that it is a constant pressure process. The non-ideal collector model does not require either of these assumptions. In the non-ideal case the fluid can enter the collector as a subcooled liquid, and exit the collector as a superheated vapor.

The primary difference between the ideal model and a real BFSC is seen by comparing the temperature profile in the collector. The temperature in the ideal model is assumed to be constant through out the entire collector. The temperature profile for a non-ideal BFSC is shown in figure 3.1.1. The bulk fluid temperature and the plate temperature are shown as a function of distance in the flow direction. Assuming a net solar gain to the collector, heat is transferred from the plate to the heat-transfer fluid in the collector. The plate temperature will be a few degrees higher than the collector due to the resistance of the collector plate and the heat transfer coefficient between the collector and fluid.

The fluid generally enters as a subcooled liquid, and is heated as it moves up the collector. The temperature of the plate and the bulk fluid temperature increase at almost a constant rate. The non-linearity of the curve is due to increases losses from the plate as the temperature increases. When the plate temperature reaches the saturation temperature of the fluid, subcooled boiling begins. The fluid near the walls of the riser tube is heated up and boils. The vapor bubbles are condensed as they move away from the wall and mix in with the colder fluid at the center of the tube. The heat transfer coefficient associated with subcooled boiling is much greater than that of the laminar fluid flow of the

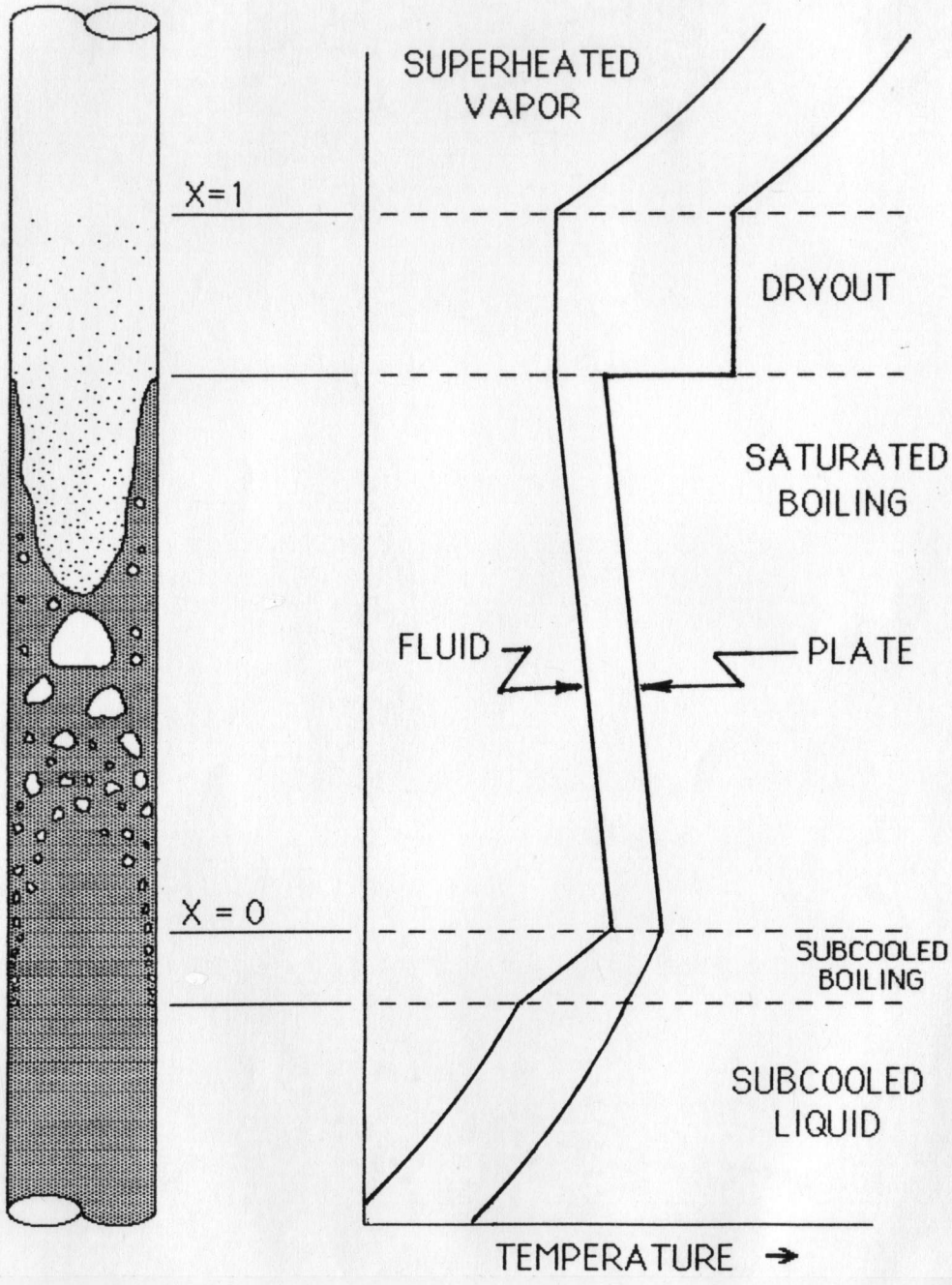

3.1.1 Temperature Profile in a Boiling Fluid Solar Collector

subcooled liquid. At this point the bulk fluid temperature begins to rise at an increased rate and the difference between the plate and the bulk fluid temperature decreases due to the higher transfer of heat to the fluid.

Saturated boiling begins when the bulk fluid temperature reaches the saturation temperature. Once boiling begins, the fluid temperature no longer increases as it moves up the collector. The fluid temperature will actually decrease slightly due to the reduced hydrostatic head and correspondingly lower fluid boiling temperature. In most cases, the variation in boiling temperature due to hydrostatic head is only a few degrees. Figure 3.1.2 shows the maximum amount of boiling point elevation due to the hydrostatic head of fluid in a collector 1.8 meters long and at a 60° slope for R-11 and R-12. ΔT_{bp} is the boiling point elevation, and T_{sat} is the saturation boiling temperature at the top of the collector. This figure demonstrates a maximum boiling point elevation since it assumes the collector is completely full of liquid refrigerant. This assumption ignores the amount of the collector in a subcooled condition and the reduced hydrostatic head due to vapor bubbles in the collector. From figure 3.1.2 it can be seen that the boiling point elevation depends on both temperature and type of refrigerant. In the results presented in this chapter, the variation in boiling temperature through the collector was

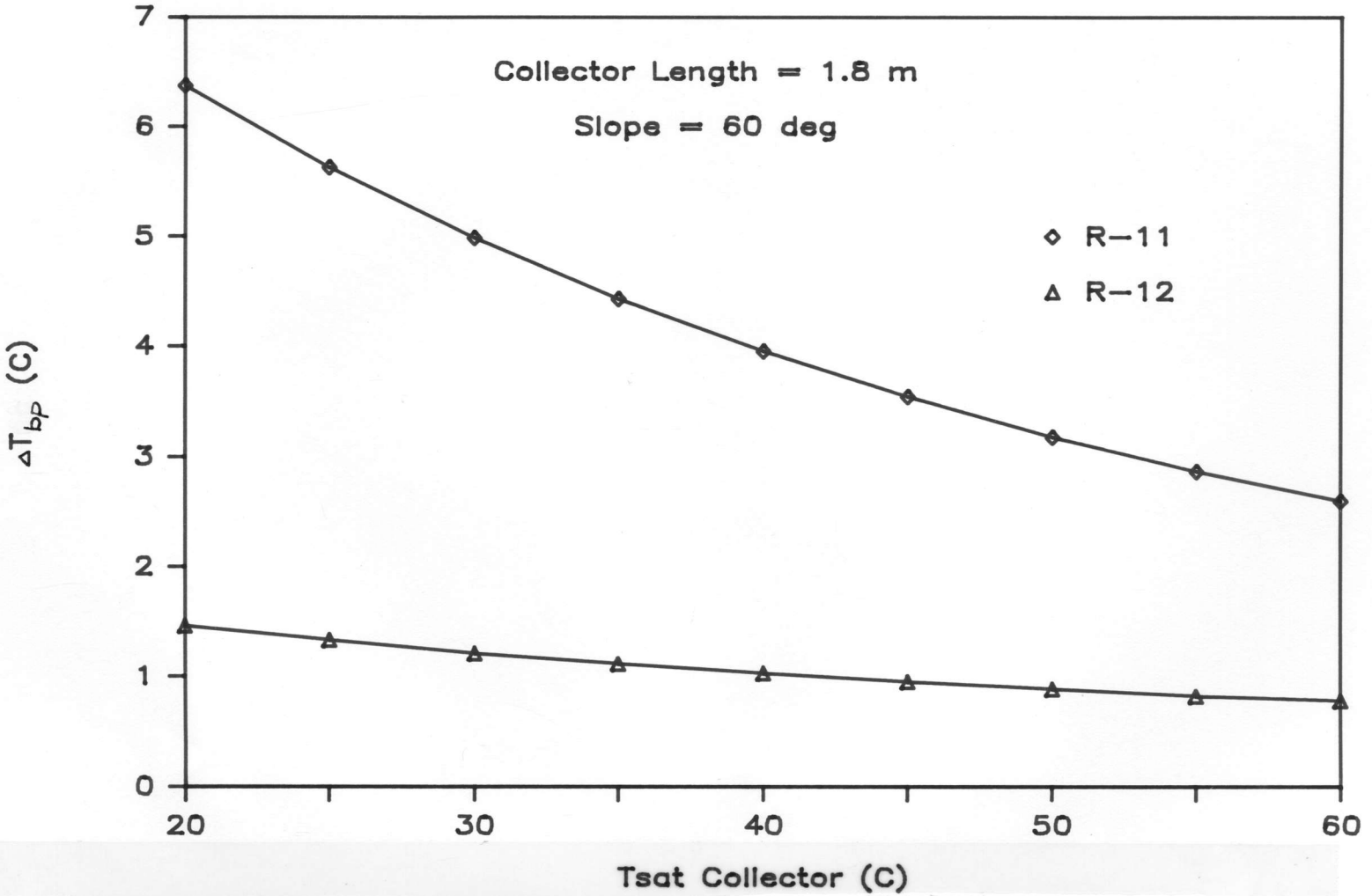

3.1.2 Boiling Point Elevation due to Hydrostatic Head of Liquid in Collector

approximately 2°C and was neglected. The temperature in the boiling section of the collector was again assumed to be constant. The heat transfer coefficient in the boiling section of the collector varies as the quality of the two-phase fluid increases; however it is usually assumed to be constant since small variations do not significantly effect the amount of heat transferred to the fluid.

Boiling heat transfer continues to occur as the quality of the two-phase fluid increases until a condition known as dryout occurs. Dryout is when the walls of the riser tube are no longer wetted by liquid refrigerant. This can occur long before the quality of the fluid reaches 1.0. This is due to the entrainment of liquid in the vapor. When dryout occurs, the heat transfer between the collector and fluid no longer relies on the boiling heat transfer coefficient. The convective gas heat transfer coefficient is much lower than the boiling heat transfer coefficient. The temperature of the vapor at the edge of the riser becomes superheated, but the bulk fluid temperature remains virtually constant until all of the entrained liquid is vaporized. The plate temperature abruptly increases at the point of dryout due to the increased resistance of heat flow.

When a quality of 1.0 is reached, the vapor begins to be superheated. The plate and bulk fluid temperatures again begin to increase as the fluid gains energy in the

collector.

Figure 3.1.3 illustrates the energy transferred to the fluid along the length of the collector. The initial heat transfer decreases in the subcooled section due to increased losses as the plate temperature increases. The heat transfer would increase in the subcooled boiling section of the collector. Heat transfer in the boiling section would be approximately constant or increase slightly due to decreasing temperature and increasing heat transfer coefficient in the boiling section. Dryout causes a rapid decrease in heat transfer, but the heat transfer remains virtually constant until superheating begins. The heat transfer again decreases when the vapor superheats, due to increased losses associated with higher temperatures.

Al-Tamimi (14) shows experimentally obtained temperatures and calculated heat transfer coefficients for the BFSC he tested. His results generally agree with the discussion presented above. In the cases presented, dryout and superheating does not occur. However, the number of temperature sensors along the plate may have been insufficient to determine if dryout actually occurred. Also, some discrepancy in his results does occur. In one case he shows the inside wall temperature to be greater than the plate temperature. It is difficult to see how any energy could be gained if this were the case.

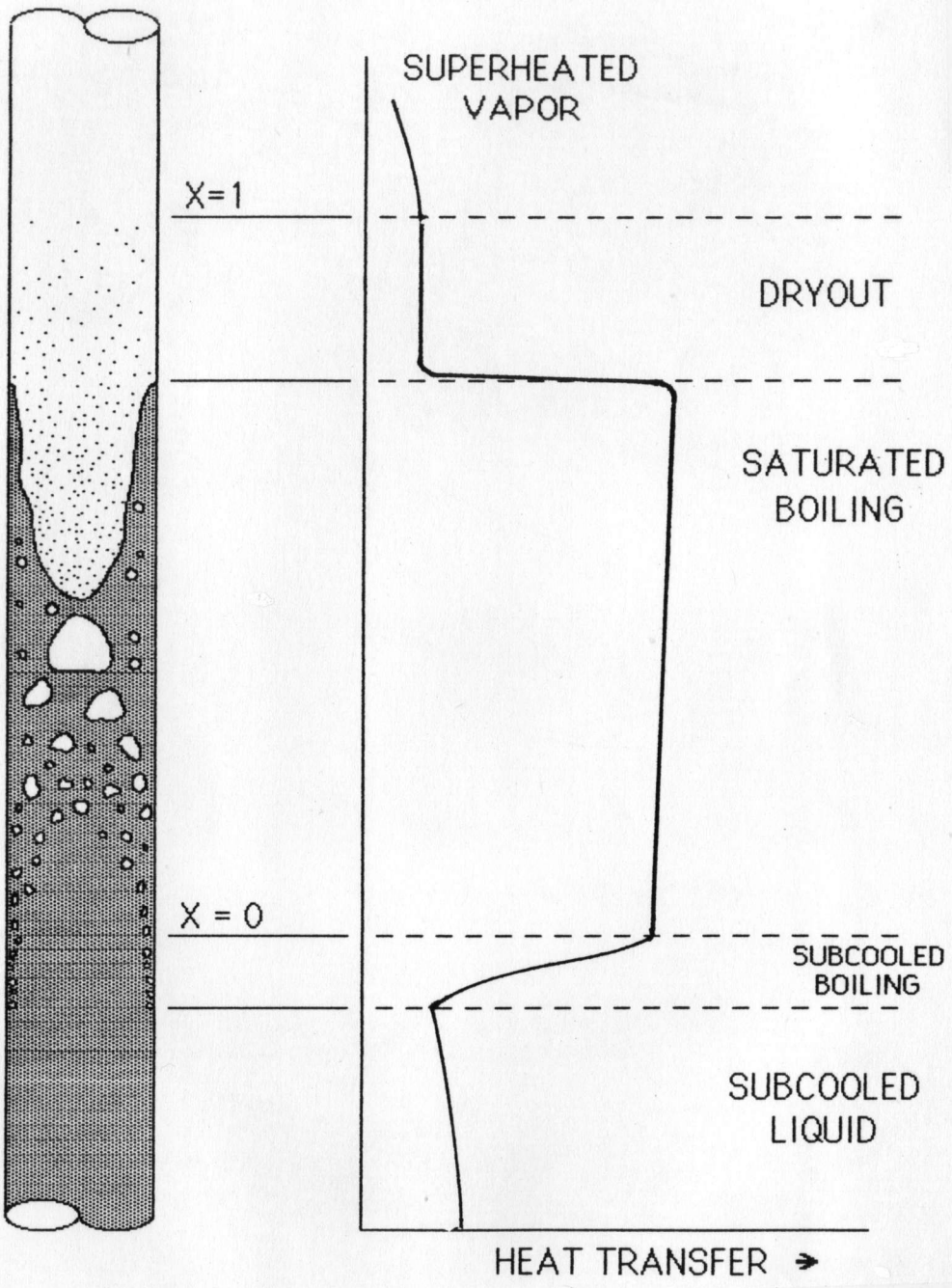

3.1.3 Heat Transfer Profile in Collector

Several approaches can be used to model boiling fluid solar collectors. The first approach might be to model it with a single equation. However, the variation in the physical processes occurring in the boiling fluid collector make this approach difficult if not impossible. The collector could be broken into differential elements and modeled. Each differential element would exist within a given realm of the boiling collector and not be split between them. Although possible this is not the most elegant approach for modeling the boiling fluid collector. A third technique is to break the collector into the different realms which occur in the collector and to model each separately. The five realms described above might be classified: subcooled, subcooled boiling, boiling, dryout, and superheated. The total energy gain in the collector can be found by adding the gains in each section. The biggest problem with this approach is in determining how much of the collector operates in each realm.

The remaining sections in this chapter discuss in detail how each of the collector sections are modeled, and what causes each to occur.

3.2 Boiling

The boiling section of the non-ideal BFSC is modeled in the same form as the ideal boiling fluid collector. The variation in boiling temperature due to pressure drops

across the collector is negligible and is again ignored here. The useful energy gain, Q_b, from the boiling section of the collector is:

$$Q_b = A_b F_{R,b} [S - U_L (T_{sat} - T_a)] \qquad (3.2.1)$$

where, A_b is the area of the boiling section of the collector. This model is very simplistic and ignores the actual processes occurring in the collector, but these will be considered in more detail in chapter 5.

3.3 Subcooled

In a boiling collector-condenser system, the fluid entering the collector is commonly in a subcooled state. As previously mentioned, the fluid must rise part way up the collector before it is heated up to its saturation temperature and begins to boil. Subcooling may occur as a result of frictional pressure drops in the collector and vapor lines, hydrostatic head of the fluid in the collector, momentum pressure drops associated with phase change in the collector, subcooling in the condenser, and heat losses in the liquid return line. All of these are discussed in later sections of this chapter, except subcooling in the condenser. Subcooling in the condenser does not appear to be significant in the system studied, which utilizes a drip style condenser. All of the energy gained in the subcooled section will be released at the

condenser except for subcooling due to heat losses.

The subcooled portions of the collector can be modeled like conventional collectors, with the exception that the exiting temperature is known. It is assumed that the amount of subcooling is known, or the physical processes which cause subcooling can be evaluated to determine the amount of subcooling. Since the inlet and outlet temperatures are known, the amount of energy which is gained in the subcooled portion of the collector is known. What is unknown, is how much of the collector is in a subcooled state. The temperature distribution in the subcooled section of the collector takes the form (21),

$$\frac{T_{sat} - T_a - S/U_L}{T_{c,i} - T_a - S/U_L} = \exp\left[- \frac{A_{sc}\ U_L\ F'}{(\dot{m}\ C_p)_{ref}} \right] \qquad (3.3.1)$$

where $T_{c,i}$ is the temperature of the subcooled liquid entering the collector, and A_{sc} is the area of the collector subcooled. A_{sc} can be rewritten:

$$Asc = A_c\ Z_{sc} \qquad (3.3.2)$$

Where Z_{sc} is the fraction of the collector's length subcooled.

Substituting for A_{sc} and solving for Z_{sc}:

$$Z_{sc} = \frac{(\dot{m}\ C_p)_{ref}}{A_c\ U_L\ F'} \ln\left[\frac{T_{c,i} - T_a - S/U_L}{T_{sat} - T_a - S/U_L} \right] \qquad (3.3.3)$$

If Z_{sc} is less than one, the energy gain in the subcooled portion of the collector can be determined using:

$$Q_{sc} = (\dot{m}\ C_p)_{ref}(T_{sat} - T_{c,i}) \qquad (3.3.4)$$

If Z_{sc} is greater than or equal to one, then the entire collector exists in a subcooled condition. In the case of a thermosyphoning system, no circulation of fluid would occur. A pumped system would work like a standard hydronic collector and heat exchanger for values of Z_{sc} greater than 1.0.

If a subcooled boiling section is to be included in the model, the same method is used as above, except that there will be two subcooled sections. The only difference between the subcooled section and the subcooled boiling section is that the latter has a higher heat transfer coefficient between the collector and the heat transfer fluid. The collector efficiency factor for the subcooled boiling section, $F'_{sc,b}$, is greater than the collector efficiency factor for the subcooled section using laminar flow heat transfer, $F'_{sc,l}$. The point at which the plate temperature reaches the saturation temperature of the fluid is where subcooled boiling begins. If the plate temperature is known then the fluid temperature in the collector can be determined.

$$T_f = T_p - \frac{1 - F'}{F'} \left[\frac{S}{U_L} + T_a - T_{sat} \right] \qquad (3.3.5)$$

When $T_p = T_{sat}$, then the temperature of the fluid at which subcooled boiling begins, $T_{sc,b}$, is found.

$$T_{sc,b} = T_{sat} - \frac{1 - F_{sc,1}'}{F_{sc,1}'} \left[\frac{S}{U_L} + T_a - T_{sat} \right] \qquad (3.3.6)$$

The area of each subcooled section can be found using (3.3.3).

$$Z_{sc,1} = \frac{(\dot{m}\, C_p)_{ref}}{A_c\, U_L\, F_{sc,1}'} \ln \left[\frac{T_{c,i} - T_a - S/U_L}{T_{sc,b} - T_a - S/U_L} \right] \qquad (3.3.7)$$

$$Z_{sc,b} = \frac{(\dot{m}\, C_p)_{ref}}{A_c\, U_L\, F_{sc,b}'} \ln \left[\frac{T_{sc,b} - T_a - S/U_L}{T_{sat} - T_a - S/U_L} \right] \qquad (3.3.8)$$

The energy gain in the subcooled sections is found using (3.3.4). It is necessary to check that $(Z_{sc} + Z_{sc,b}) < 1.0$. If $T_{sc,b} < T_{c,i}$ then the entire subcooled region utilizes subcooled boiling heat transfer.

The two subcooled sections of the boiling fluid collector could also be considered to be two collectors in series. It is possible to combine two collectors in series and define new values for $F_R\,(\tau\alpha)$ and $F_R\, U_L$ for the combination (21). In the case of the boiling collector, $(\tau\alpha)$ and U_L are essentially constant, thus only a new F_R needs to be defined for the combined sections.

$$F_R = \frac{A_1 F_{R1} (\tau\alpha)_1 (1 - k) + A_2 F_{R2} (\tau\alpha)_2}{A} \qquad (3.3.9)$$

$$F_{R,sc} = Z_{sc,1} F_{R,1} (1 - K) + Z_{sc,b} F_{R,b} \qquad (3.3.10)$$

$$K = \frac{A_c Z_{sc,b} F_{R,b} U_L}{\dot{m} C_p} \qquad (3.3.11)$$

If only subcooled and boiling sections are present in the BFSC, then the energy balance for the boiling collector-condenser system can be written:

$$Q_b + Q_{sc} = Q_{cond} \qquad (3.3.12)$$

when the subcooled energy gain is recovered at the condenser. This would be the case for subcooling due to pressure drops, or subcooling in the condenser. For the case where the subcooled energy gain is not recovered at the condenser, as in the case of pipe losses form the liquid return line, the energy balance on the collector-condenser system can be written:

$$Q_b = Q_{cond} \qquad (3.3.13)$$

In actual practice a portion of the energy gain in the subcooled section is retrieved and a portion is not. The energy gain in the boiling section, Q_b, is found using (3.2.1), where:

$$A_b = (1 - Z_{sc})\, A_c \qquad (3.3.14)$$

Z_{sc} is found using (3.3.3), and the mass flow rate of refrigerant is found using:

$$\dot{m}_{ref} = Q_b / h_{fg} \qquad (3.3.15)$$

The energy gain in the subcooled section is found from (3.3.4). The energy retrieved in the condenser is found using equations (2.2.2) and (2.2.3).

To solve these equations it is necessary to know how much subcooling exists in the collector. Figures 3.3.1 illustrates how the collector-condenser system efficiency change for various levels of subcooling (ΔT_{sc}). The energy gain in the subcooled section is not included in figure 3.3.1. It is important to note that the efficiency is plotted against $(T_i - T_a) / G_T$, where T_i is the condenser inlet water temperature, and not the temperature of the fluid entering the collector. Also notice that the efficiency for various levels of subcooling is not a linear relationship. Figure 3.3.2 is an enlargement of figure 3.3.1, for ΔT_{sc} = 30°C. Notice, that for a given amount of subcooling, the efficiency appears to be linear for different levels of solar radiation. The reduction in collector-condenser system efficiency does not appear to be significant for small values of subcooling (5 - 10°C).

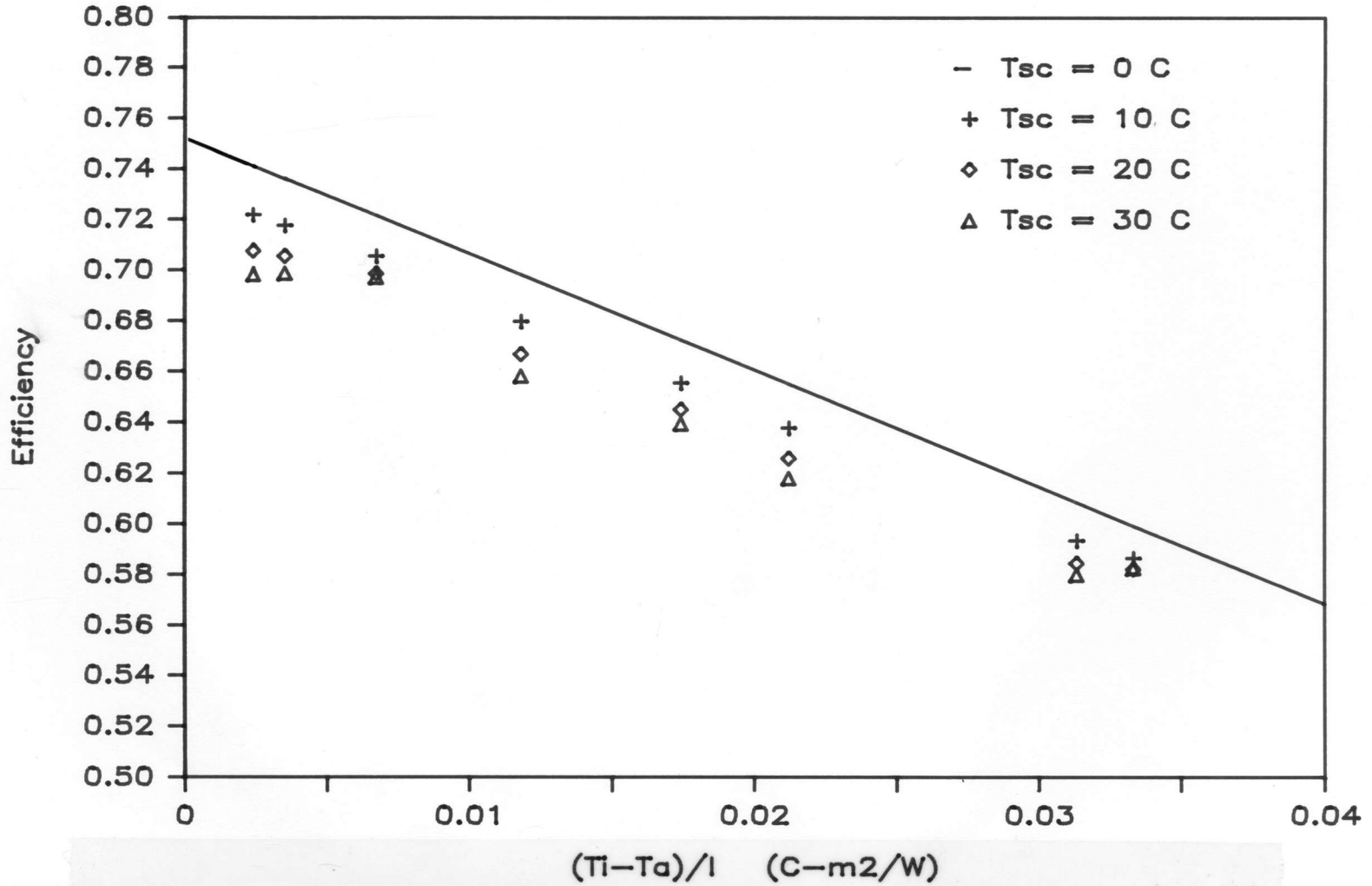

3.3.1 Instantaneous Thermal Efficiency for BFSC with Subcooled Liquid Entering

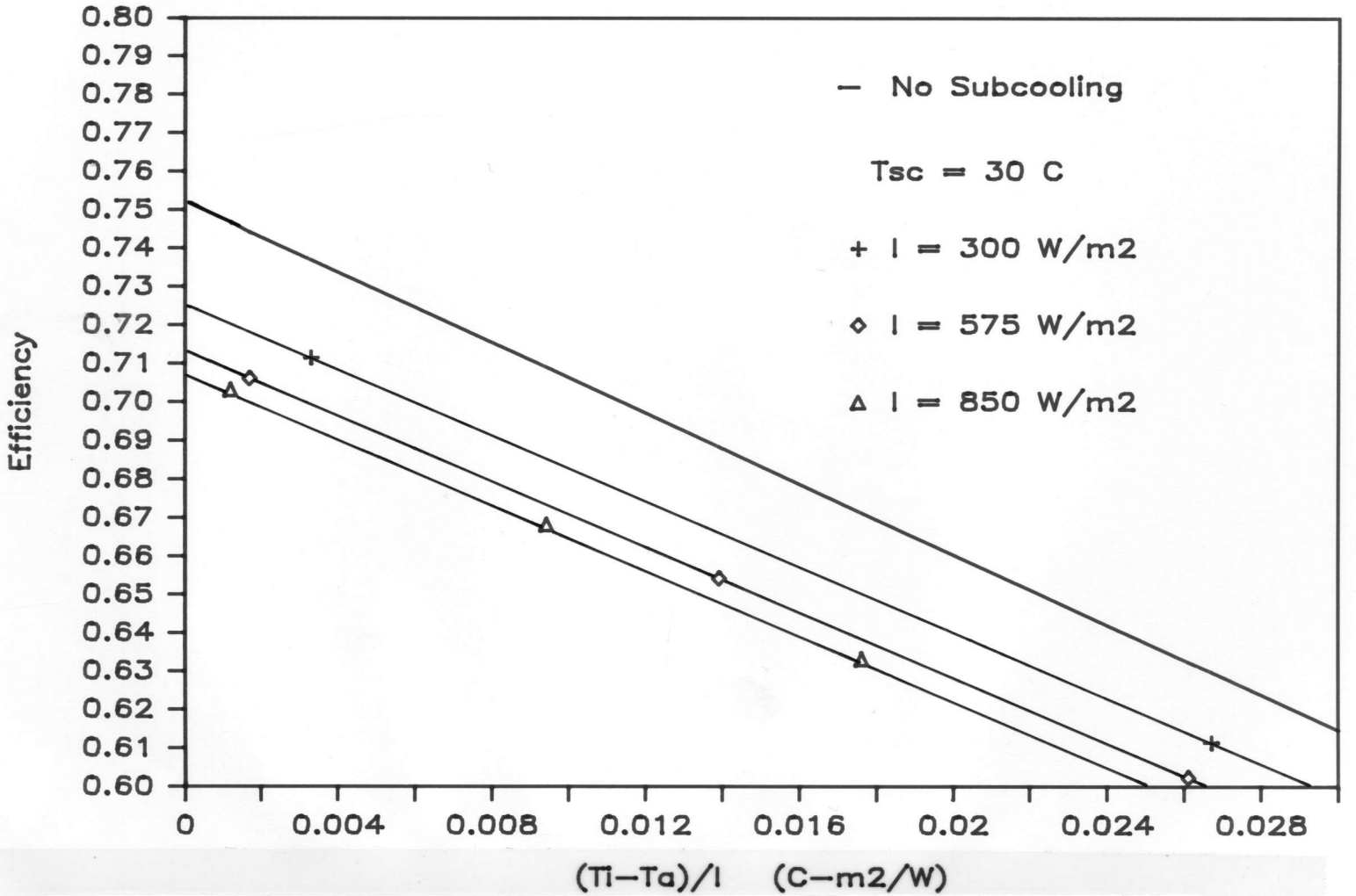

3.3.2 Solar Radiation Dependence on Thermal Efficiency of Collector with Subcooling

3.4 Dryout and Superheating

Dryout and superheating are two undesirable conditions which may occur in boiling fluid solar collectors. Dryout occurs when a portion of the collector riser tube is not wetted by liquid refrigerant. Thus, the high boiling heat transfer coefficient is replaced by a much lower gas heat transfer coefficient and the plate temperature will increase abruptly at the point of dryout. The bulk fluid temperature will remain constant as long as the quality is less than 1.0. When the vapor quality reaches 1.0, any additional heat added will superheat the vapor. Dryout is not desirable since it reduces collector efficiency by increasing the collector plate temperature and reducing F_R.

Dryout is most likely to occur at times of very low or very high solar radiation. During times of low solar radiation, the mass flow rate of refrigerant is insufficient to wet the upper portion of the collector. Since the collectors are not completely filled with liquid refrigerant, they rely on the turbulence and effective density change of boiling to wet the top of the collector. At high levels of solar radiation, the mass flow rate of refrigerant is again not sufficient to wet the entire collector due to the friction in the collector, and liquid refrigerant lines which restricts the flow of liquid refrigerant.

In most situations it is difficult to know when dryout will occur, due to the complexity of the boiling process occurring in the collector. The quality and location at which dryout occurs is a function of temperature, solar radiation, wind speed, and the temperature of the water entering the condenser. The complexity of the mechanism which causes dryout also makes it difficult to develop a model which will predict it. Superheating is also difficult to model in a thermosyphoning boiling collector, since it may occur along with dryout. The approach taken here is to develop a model which determines the effect on collector-condenser system efficiency for known amounts of dryout and superheating. A more detailed analysis of the fluid dynamics is required to develop a model which can predict the point at which dryout occurs.

The dryout section of the collector can be modeled in the same manner as the boiling section of the collector. During dryout the collector exists in a two-phase condition, thus the bulk fluid temperature will remain essentially constant. The only difference between dryout and saturated boiling is the lower heat transfer coefficient between the riser tube and the fluid.

$$Q_d = A_d F_{R,d}[S - U_L (T_{sat} - T_a)] \qquad (3.4.1)$$

Where, A_d is the area and $F_{R,d}$ is the heat removal factor for the dryout section of the collector. Since the boiling

and dryout sections are assumed to be at the same constant temperature (T_{sat}), it is possible to combine them into a single equation.

$$Q_{b+d} = (A_b F_{R,b} + A_d F_{R,d}) [S - U_L (T_{sat} - T_a)] \quad (3.4.2)$$

The superheated section of the collector is modeled like a standard collector with a reduced area A_{sh} and a collector heat removal factor $F_{R,sh}$.

$$A_{sh} = A_c Z_{sh} \quad (3.4.3)$$

$$F_{R,sh} = \frac{(\dot{m} C_p)_{ref}}{A_{sh} U_L} \left(1 - \exp\left[- \frac{A_{sh} U_L F'}{(\dot{m} C_p)_{ref}}\right]\right) \quad (3.4.4)$$

$$Q_{sh} = A_{sh} F_{R,sh} [S - U_L (T_{sat} - T_a)] \quad (3.4.5)$$

Where, Z_{sh} is the length of the collector which is in a superheated state. Figures 3.4.1 illustrates how the instantaneous efficiency of a BFSC is reduced by superheating. Dryout has the same effect as superheating, however the reduction in efficiency is not as large.

If significant portions of the collector exist in a dryout or superheated state the collector-condenser system efficiency is dramatically reduced. For the collector-condenser system tested in this study, dryout and superheating do not appear to be significant (12,14) and

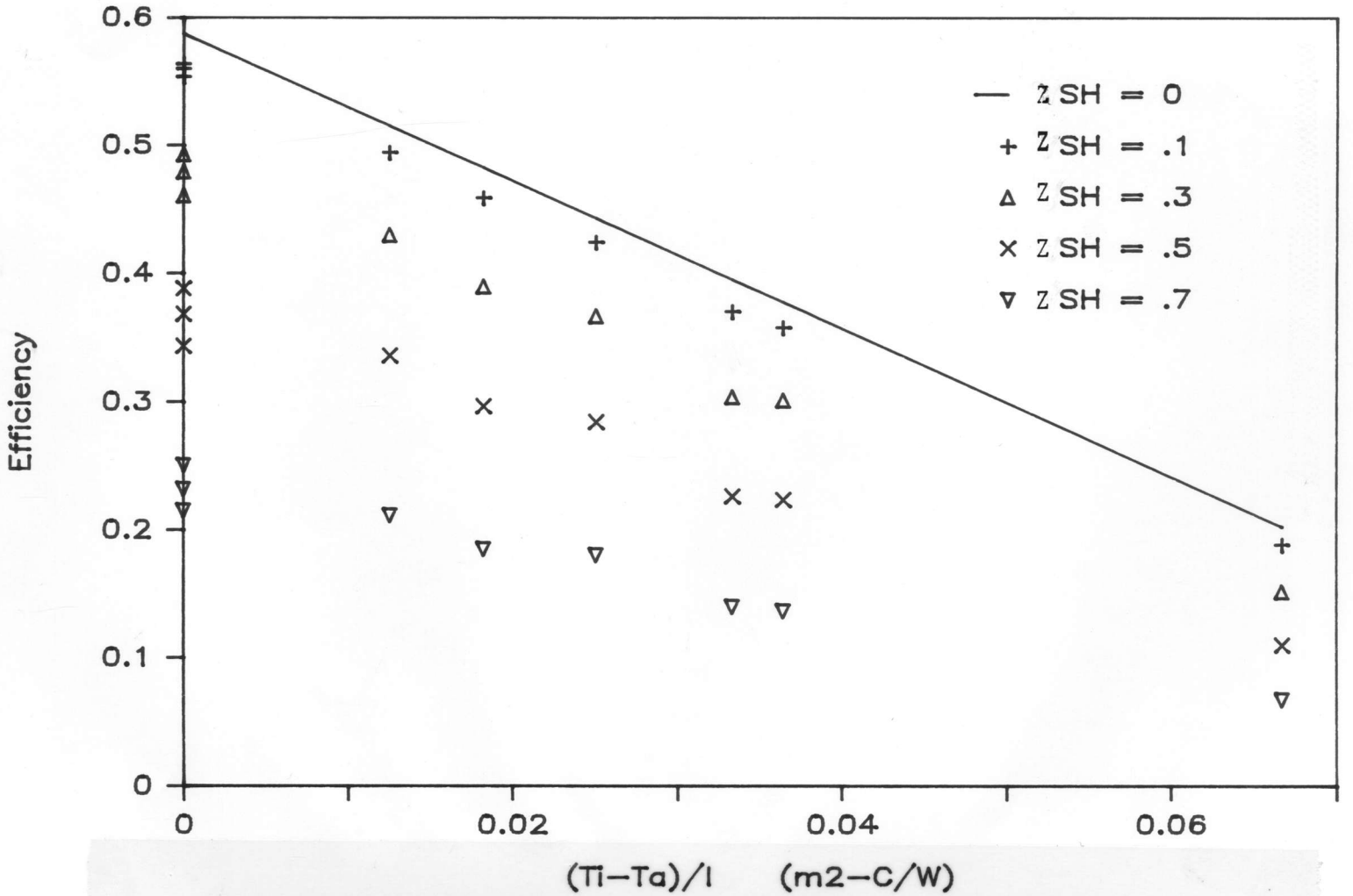

3.4.1 Instantaneous Thermal Efficiency of BFSC with Superheating

are not considered.

3.5 Pressure Drops

In a standard hydronic collector system, pressure drops around the collector loop have very little effect on the system except in choosing a pump. Larger pumps will increase the parasitic energy requirements of the system, but have very little effect on the system performance. Pressure drops in a BFSC system however can adversely effect the operation and efficiency of the system. Pressure drops result from three main causes: the hydrostatic head of the fluid, frictional pressure drop in the collector and pipes, and kinetic energy variations due to velocity changes associated with phase change. The location of the pressure drop dictates the effects it will have on system operation. Pressure drops occur in three locations: the vapor line, the liquid return line, and the collector. Generally the pressure drop in the condenser is small and can be ignored.

Friction is the main cause of pressure drops in the vapor line. Friction in the vapor line has three noticeable effects on the system. First, the pressure difference between the collector and condenser will result in the vapor entering the condenser in a superheated state, assuming no thermal losses. The rate of heat transfer in the condenser will thus be reduced compared to the ideal

case with no pressure drop. For a given rate of heat transfer in the condenser, the average collector temperature increases with increasing pressure difference between the collector and condenser which lowers the collection efficiency. A second effect of friction in the vapor line that is the additional height of liquid in the return line necessary to offset the friction and maintain the circulation of the refrigerant. The condenser should be located far enough above the collector such that it will not be flooded by the additional liquid head. The displacement of fluid from the collector to the liquid return line may cause "dry out" conditions in the collector. A third effect of friction in the vapor line is that the fluid entering the collector will be subcooled due to the lower saturation temperature in the condenser.

Pressure drops in the vapor line due to friction are accounted for using:

$$-\Delta P_{f,vl} = \frac{f \rho L V^2}{(2 d_{vl}).} \qquad (3.5.1)$$

where the friction factor f, is determined using the following correlation (22) for turbulent flow in smooth pipes:

$$1 / \sqrt{f} = 0.87 \ln(Re_D \sqrt{f}) - 0.8. \qquad (3.5.2)$$

Figure 3.5.1 illustrates how system efficiency drops off when the vapor line diameter is decreased. The figure was generated using the base system with a solar radiation intensity of 800 W/m^2 and a pipe length of 10 m. The effect of friction can also be seen by increasing the length of the vapor line. Figure 3.5.2 shows the system efficiency for various vapor line lengths and with a diameter of 0.0141 m. Longer vapor pipes have increased friction which result in reductions in system efficiency. In figures 3.5.1 and 3.5.2, thermal capacitance effects, heat losses from the vapor line, and the hydrostatic head of the vapor were not included. The reduction in system efficiency would have been far greater in figure 3.5.2 if they had. Figure 3.5.3 illustrates how the instantaneous efficiency is a function of solar radiation, for a single collector with a vapor line length of 10 m and diameter of 0.0141 m. The top curve is for the case of no vapor line friction. When $(T_i - T_a)/I$ is decreased, the deviation from the no friction case efficiency increases. Also, the larger the solar radiation intensity, the larger the reduction in system efficiency. The major reason for this behavior is that the mass flow rate of refrigerant in the collector-condenser system is both a function of $(T_i - T_a)/I$ and the intensity of solar radiation. At high solar radiation intensities or low $(T_i - T_a)/I$, the mass flow rate of refrigerant in the vapor line is high, thus causing

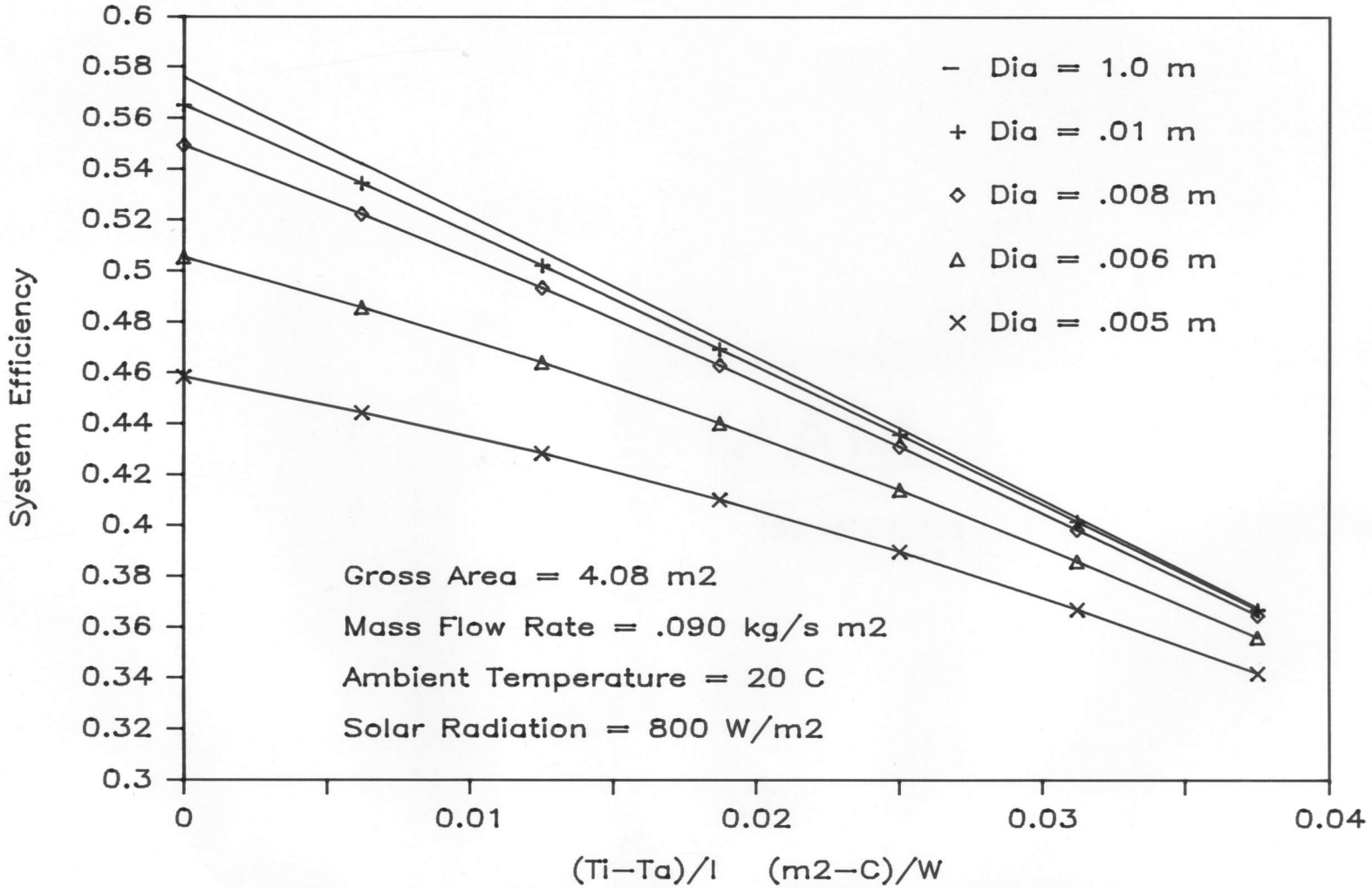

3.5.1 Effect of Friction on BFSC System Efficiency for Various Vapor Line Diameters

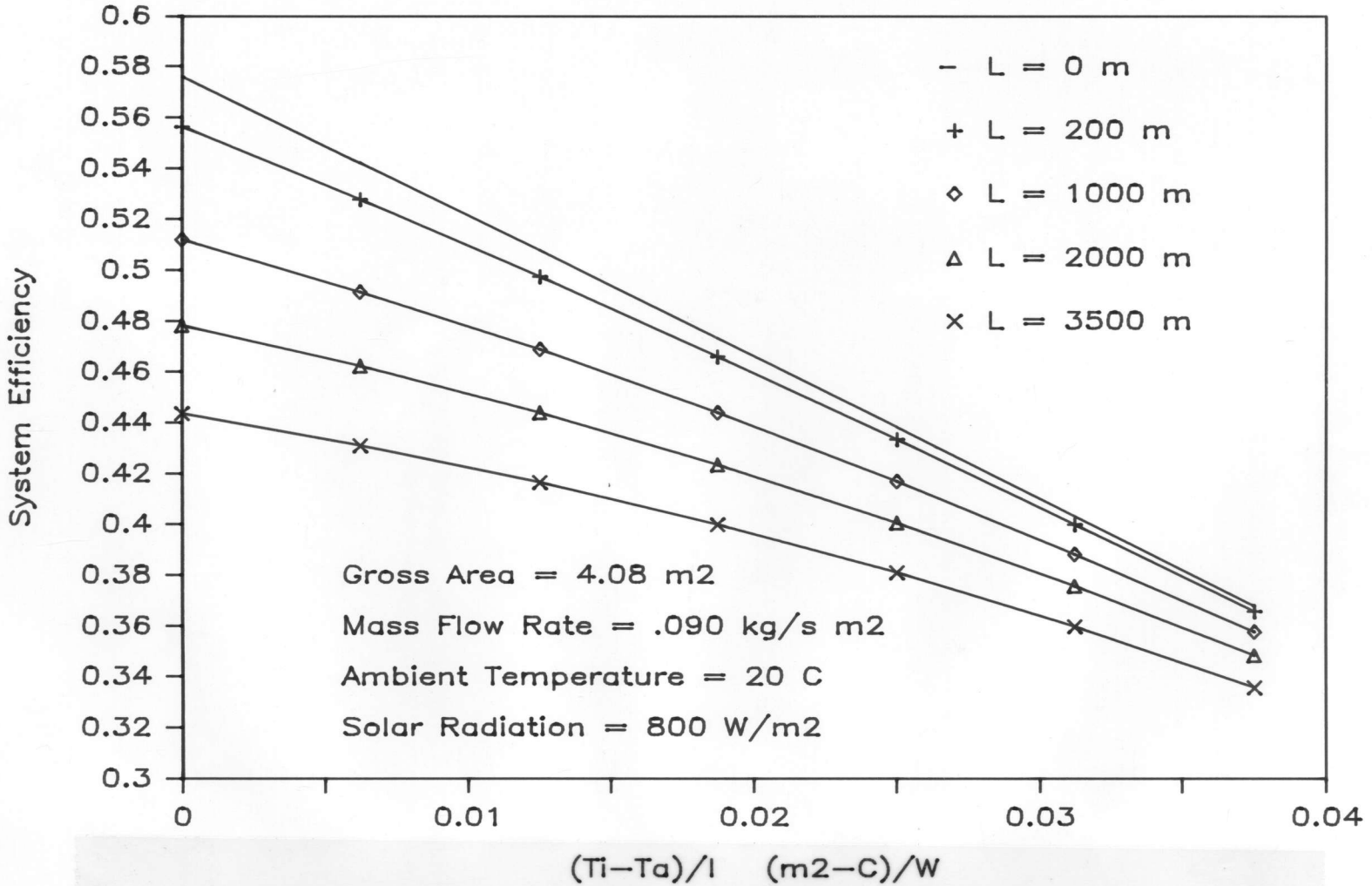

3.5.2 Effect of Friction on BFSC System Efficiency for Various Vapor Line Lengths

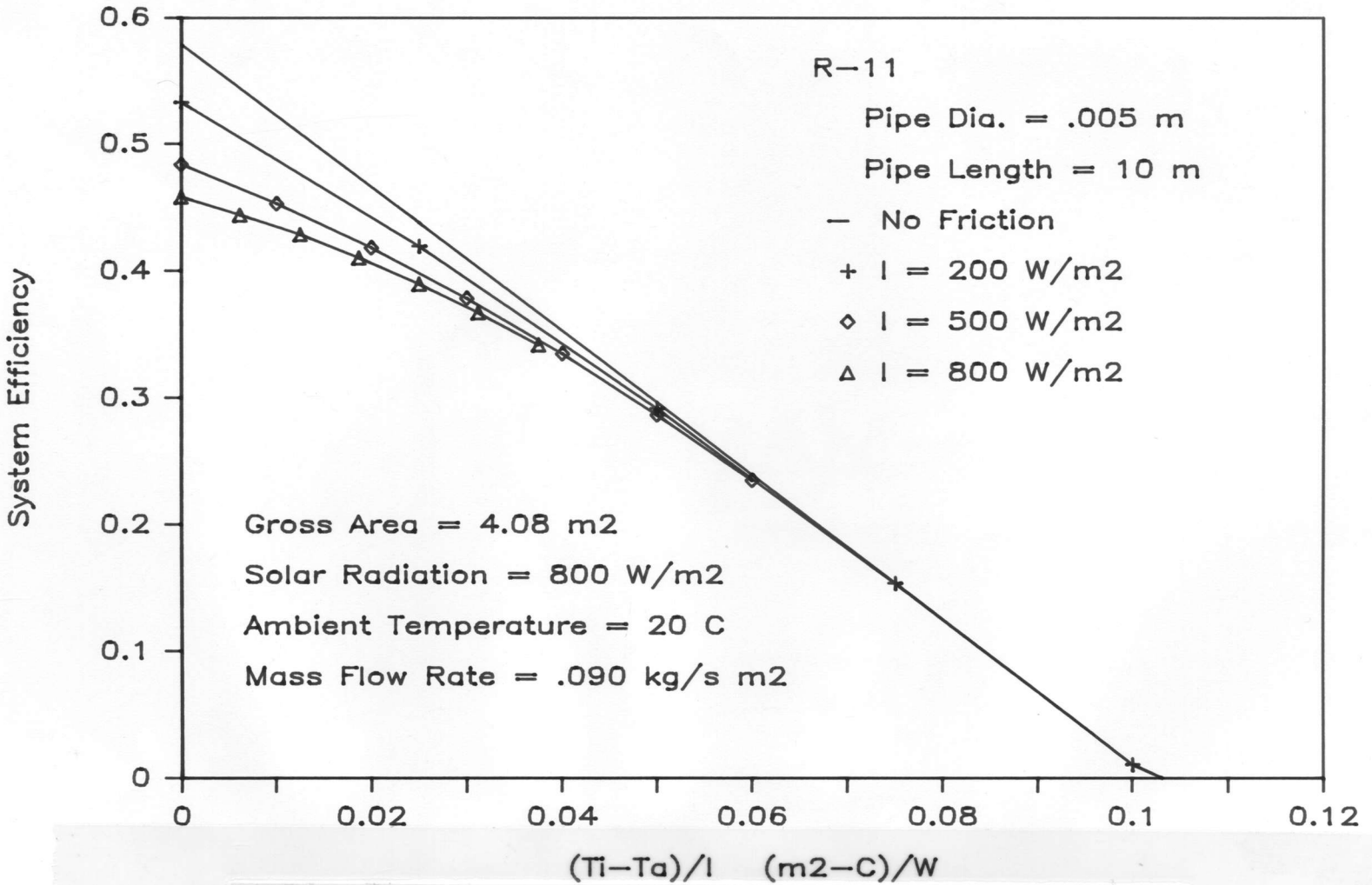

3.5.3 Solar Radiation Dependence of Thermal Efficiency for BFSC with Friction in the Vapor Line

increased friction and reduced efficiency.

In the systems considered for figures 3.5.1 - 3.5.3, the hydrostatic head in the liquid return line necessary to overcome the frictional pressure drop between the collector and condenser was sometimes as large as 15 m, as a result of unrealistic vapor line lengths or diameters examined. In a real system system, the pressure drop between the collector and condenser would be limited by the physical height of the condenser above the collector. If the pressure drop in the vapor line is large, the condenser may flood. There will also be a net transport of liquid from the collector to the liquid return line which may cause collector dryout or superheating. If the physical configuration of the system does not allow the hydrostatic head to get this large, then the collector-condenser system will adjust such that a new equilibrium condition is met at a higher collector temperature and a lower refrigerant mass flow rate. In this case the pressure drop would be equal to the maximum hydrostatic head possible in the liquid return line.

The main causes of pressure drops in the liquid return line are friction and the hydrostatic head of the liquid. The major effect of friction in the return line is the hydrostatic head of liquid that will be necessary to overcome the friction. This will not cause any subcooling at the collector inlet because the pressure increase due to

the liquid hydrostatic head is equal to the pressure drop caused by friction. However, if the hydrostatic head of the liquid is not enough to offset the friction in the liquid return line, superheating may result due to insufficient fluid entering the collector. The pressure drop associated with the hydrostatic head of the liquid in the liquid return line is calculated,

$$\Delta P_{stat,l} = \rho_f \, g \, L_l \qquad (3.5.3)$$

Frictional pressure drops in the liquid return line evaluated using (3.5.1) and the properties of the liquid refrigerant and the liquid return line. The friction factor, f, is for laminar flow:

$$f = 64 \; / \; Re_D \qquad (3.5.4)$$

There are three causes of pressure drops in the collector: friction, hydrostatic head, and the momentum change of the fluid. The largest momentum pressure drop in the collector is due to the velocity increase caused by the fluid changing phase. The momentum pressure drop is small compared to the pressure drop associated with the hydrostatic head and friction. The momentum pressure drop is not included in the model developed in this chapter but is included in chapter 5. The hydrostatic head of the fluid in the collector can be found using:

$$\Delta P_{stat} = \bar{\rho}\, g\, L_c \sin\beta \qquad (3.5.5)$$

Where, $\bar{\rho}$ is the average density of the refrigerant in the collector. If frictional and momentum pressure drops around the collector loop are small then the static head in the collector can be approximated:

$$\Delta P_{stat} = (s - Z_{sc})\, \rho_f\, g\, L_c \sin\beta \qquad (3.5.6)$$

Where, s is the initial fill of the collector and ρ_f is the density of the liquid at the time of fill.

Friction in the collector results in effects similar to friction in the vapor and liquid return lines. There will be a larger pressure drop across the collector, than the no friction case, and thus more subcooling of the collector inlet fluid. The vapor entering the condenser may be superheated due to dry-out caused by the restriction of flow in the collector.

In the situations mentioned above, friction has a negative effect on the efficiency of the boiling collector-condenser system. A well designed system should attempt minimize frictional effects.

3.6 Heat Losses

Energy losses in the collector-condenser loop will have different effects on the system depending on where they occur. Losses in the collector are accounted for in the collector overall energy loss coefficient, U_L, in the collector efficiency equation. Heat transfer from the vapor line will cause liquid to condense in the line and flow back to the top of the collector. Ignoring pressure drops in the line, this condensation occurs at a constant temperature and these losses take the form:

$$Q_{loss,vl} = UA_{vl} (T_{boil} - T_a) \tag{3.6.1}$$

Beckman(23) showed that these losses can be included in the collector equation by defining a new collector loss coefficient U_L':

$$U_L' = U_L + \frac{UA_{vl}}{(1-Z^*) A_c F_R} \tag{3.6.2}$$

Where Z^* is the fraction of the collector which is not boiling. Losses which occur in the liquid return line cannot be included in the boiling collector equation because they cause subcooling of the liquid. Liquid line losses can be determined using:

$$Q_{loss,rl} = UA_{rl} \Delta T_{LMTD}$$

$$\simeq UA_{rl} (T_{c,i} - T_a) \tag{3.6.3}$$

The amount of subcooling can be determined using:

$$\Delta T_{sc} = \frac{Q_{loss,l}}{(\dot{m}\ C_p)_{ref}} \qquad (3.6.4)$$

Losses from the condenser jacket, vapor line and liquid return line to the heated space can be accounted for in a similar fashion.

Figure 3.6.1 illustrates how heat losses from the vapor line would effect the efficiency of an ideal BFSC. Note the effect looks like U_L has been increased (ie. the slope of the efficiency curve has been increased). Figure 3.6.2 illustrates the effect of heat losses from the liquid return line. The resulting effect is not as clear as the previous case, but liquid line losses basically result in a reduction of collector area. Liquid line losses cause a portion of the collector to be subcooled, and the energy gain in this section is not recovered at the condenser.

3.7 Condenser Model

The condenser modeled in this work is representative of the type in use in the marketplace. The condenser is external to the collector, and is a simple coiled heat exchanger. Several assumptions are made to simplify the analysis to the condenser. First, superheating of the vapor entering the condenser does not reduce the heat

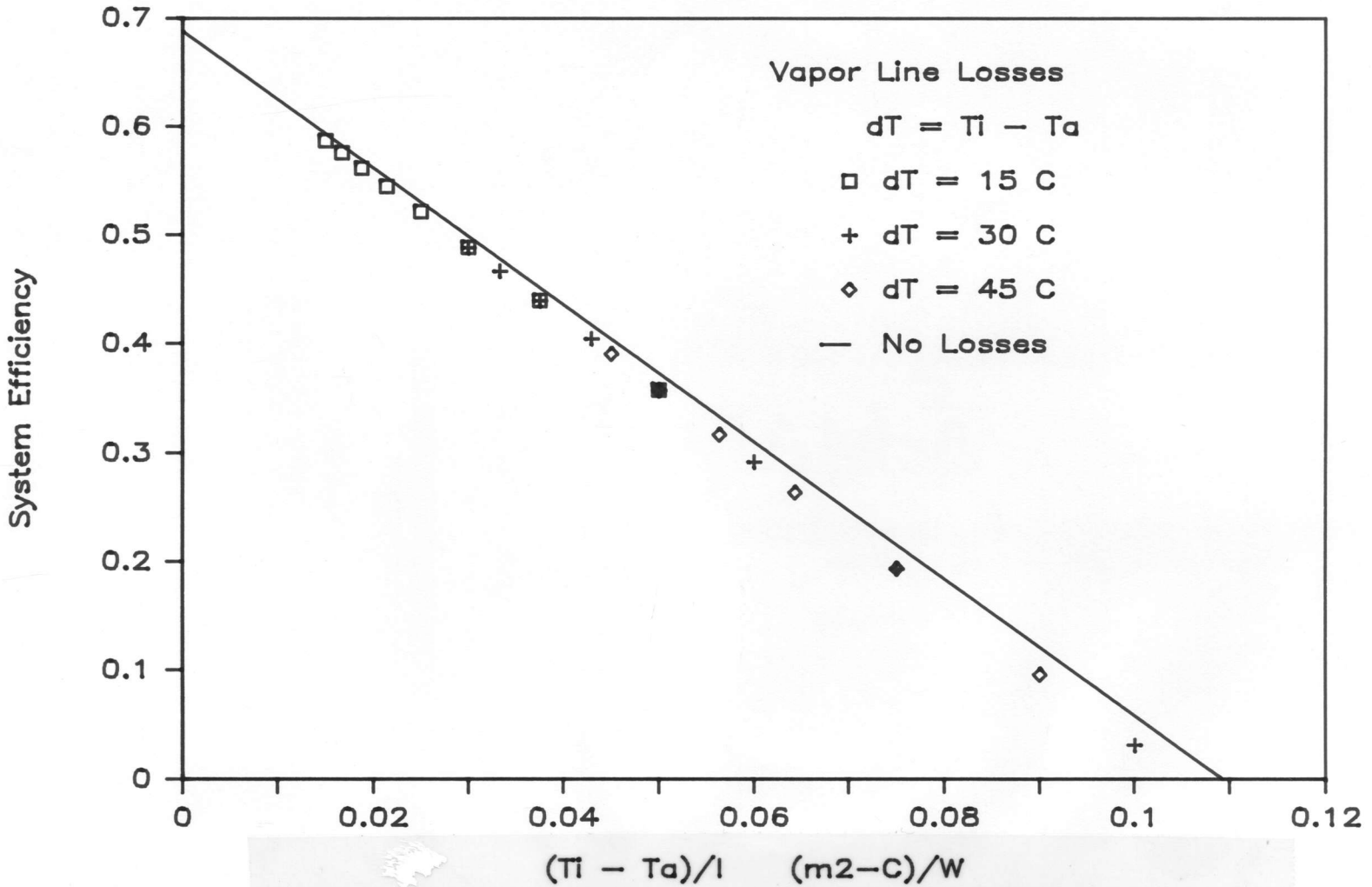

3.6.1 Effect of Heat Losses in Vapor Line on Instantaneous System Efficiency

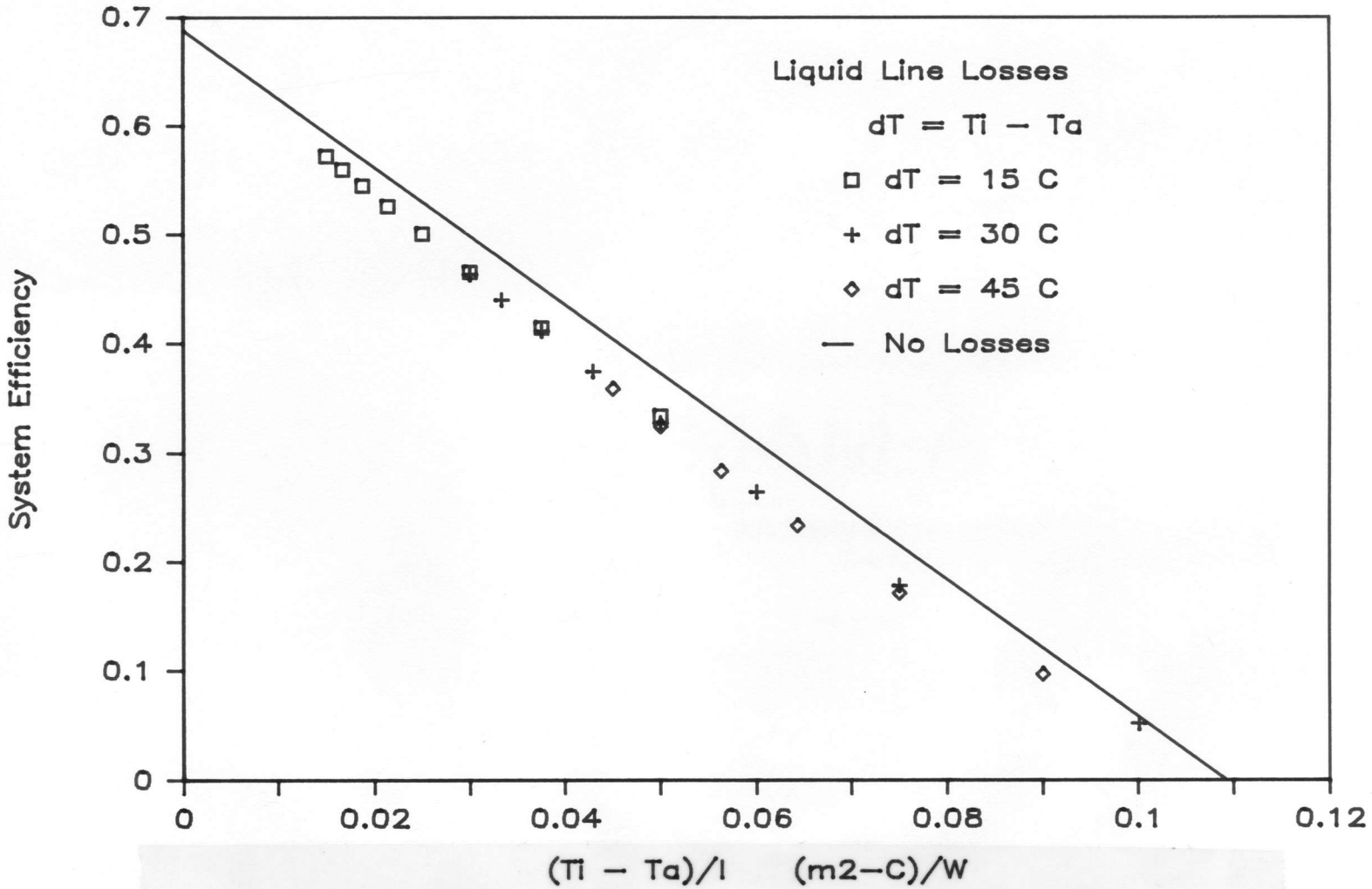

3.6.2 Effect of Heat Losses in liquid Return Line on Instantaneous System Efficiency

transfer coefficient in the condenser. Second, the condensed liquid does not get subcooled by the condenser. However it is possible for the liquid to become subcooled due to heat losses from the condenser. The condenser is modeled as a standard heat exchanger. The energy transfer in the condenser can be represented using a log mean temperature difference,

$$Q_{cond} = UA\,\Delta T_{LMTD}$$

$$Q_{cond} = \frac{UA\left[(T_{sat} - T_o) - (T_{sat} - T_i)\right]}{\ell n\left(\frac{T_{sat} - T_o}{T_{sat} - T_i}\right)} \qquad (3.7.1)$$

Where T_{sat} is the saturated boiling temperature in the collector and condenser, T_i is the temperature of the water entering the condenser, and T_o is the temperature of the water leaving the condenser. The heat transfer in the condenser can also be written:

$$Q_{cond} = (\dot{m}\, C_p)_W (T_o - T_i) \qquad (3.7.2)$$

Where $(\dot{m}\, C_p)_W$ is the mass capacitance rate of the water in the condenser. A third equation can be used to determine the mass flow rate of refrigerant around the collector-condenser loop,

$$Q_{cond} = W\,(i_{fg} + \Delta T_{sh}\, C_{p,g})_{ref} \qquad (3.7.3)$$

The condenser UA is found using,

$$\frac{1}{UA} = \frac{1}{A_c \ \eta_c \ h_c} + R_t + \frac{1}{A_h \ \eta_h \ h_h} \qquad (3.7.4)$$

The resistance associated with the copper tube, R_t, is assumed to be zero. The subscripts h and c refer to the hot and cold sides of the heat exchanger. η is the total surface temperature effectiveness (22) which is found using,

$$\eta = 1 - A_f/A_t \ (1 - \kappa) \qquad (3.7.5)$$

A_f is the exposed area of fins, A_t is the total exposed area of fins, and κ is the fin effectiveness. The convective heat transfer coefficient on the cold or water side of the condenser is found using a simplified correlation for forced convection of water (24), which accounts for temperature and velocity effects of the water.

$$h_c = \frac{150 \ (1 + .011T) \ V^{.8}}{d^{.2}} \qquad (3.7.6)$$

Where the temperature, T, is in °F; the velocity, V, is in ft/s; the inside diameter, d, is in inches, and h_c is in Btu/hr ft^2 C. Equation (3.7.6) is only valid for temperatures in the range of 40 to 220 °F. The condensation heat transfer coefficient, h_h, is found using the following correlation (25):

$$h_h = .951 \left[\frac{\rho(\rho_f - \rho_g)\, g\, K_f^3}{\mu_f\, \Gamma_z} \right]^{1/3} \qquad (3.7.7)$$

where Γ_z is the mass flow rate of condensate per unit tube length. The coiled condenser is modeled as 2 horizontal pipes, one above the other, to account for the effect of condensate on the top of the coil running down on the lower half of the coil. To model two pipes, one above the other the heat transfer coefficient is modified using:

$$h_{h,2} = h_{h,1}(1/2)^{1/4} \qquad (3.7.8)$$

3.8 Solution Technique

The basic structure of the non-ideal boiling fluid collector-condenser model is an energy balance which assumes a quasi-equilibruim state such that the energy gain in the collector equals the energy transfer to the water in the condenser plus the heat losses from the connecting pipes. If heat losses are included for the vapor and liquid return lines the basic energy balance for the collector-condenser model becomes:

$$Q_{sc} + Q_{sc,b} + Q_b + Q_d + Q_{sh} - Q_v - Q_l - Q_{cond} = 0 \qquad (3.1.1)$$

Where, Q_{sc}, $Q_{sc,b}$, Q_b, Q_d, and Q_{sh} are the energy gained in the subcooled, subcooled boiling, boiling, dryout and superheated sections of the collector, and Q_v, Q_l, and Q_{cond} are the energy losses in the vapor and liquid return

lines and the energy transferred to the water in the condenser.

It is possible to combine the equations developed in this chapter to form a single equation for the useful energy gained in a non-ideal BFSC, just as was done for the ideal collector model. However, the resulting equation can not be independently solved for the useful energy gain in the collector. The simplest solution technique is to use an iterative scheme to solve the equations. A secant method was used to solve for the useful energy gain. The temperature in the collector is guessed, then the heat losses from the pipes can be determined, which give the amount of subcooling in the collector. The energy gain in the collector can then be determined. The mass flow rate of refrigerant in the pipes can then be determined which specifies the amount of friction in the pipes, and collector. Friction also effects the amount of subcooling. A secant method is used to determine the amount of subcooling of the given temperature. If the temperature is known, then the amount of energy gained in the condenser can also be determined. A second secant method is used to adjust the temperatures in the collector and condenser until the energy balance above is satisfied.

If friction is not considered then the solution procedure is simplified. The equations developed in section 3.3 can be used in conjunction with the equations

in section 3.6. However, a secant method is still required since it is not possible to directly solve for Q_{cond}.

3.9 Property Variations

The model developed in this chapter can account for property variations with temperature. A quadratic interpolation of tabular data from (24) is used to determine density, viscosity, conductivity, specific heat and the heat of vaporization of the fluid. A variation of the Clausius-Claperyon (26) equation is used to account for boiling temperature variation due to fluctuations in pressure due to friction and the hydrostatic head of the fluid. For example the temperature in the condenser can be determined if the pressure in the condenser and the temperature and pressure in the collector are known.

$$T_{cond} = T_{sat} + \frac{RT_{sat}^2}{i_{fg}} \ln\left(\frac{P_{cond}}{P_{sat}}\right) \qquad (3.9.1)$$

Vapor pressures are calculated using an equation developed by Martin (27).

$$\log P_{sat} = A + B/T + C\log T + DT + E(F-T)/T \log(F-T) \qquad (3.9.2)$$

Where A, B, C, D, E, and F are coefficients, unique for each refrigerant. The coefficients for many refrigerants are found in reference (28). Appendix D includes a listing of the property interpolation program and the vapor

pressure calculation.

3.10 Other Boiling Collector Systems

The model developed in this chapter can be applied to a number of boiling fluid collector-condenser system configurations. The BFSC model is set up to model external condenser configurations, but collectors with the condenser located inside the collector can also be modeled by setting the vapor and liquid pipe lengths to zero. Systems using pumps in the refrigerant loop are a simplification of the model presented in this chapter, since the mass flow rate of refrigerant in the collector is a known value. However, pumped systems are more likely to have subcooling or superheating occur in the collector, due to the inability of the pump controller to adjust the refrigerant mass flow rate in the collector. Evacuated tubular heat pipes are another form of boiling fluid solar collectors. They cannot be modeled using the equations above since their efficiency is not only a function of $(T_i - T_a)/G_T$.

3.11 Summary

This chapter discussed the differences between the ideal and the non-ideal boiling fluid solar collector models. The causes and the effects of subcooling, dryout, and superheating were discussed. Models were developed to determine their effect on collector-condenser system efficiency. The effects of pressure drops due to friction

and the hydrostatic head of the fluid, and heat losses from the connecting pipes were modeled and the magnitude of their effect on system performance was also determined.

4. SYSTEM STUDIES

This chapter presents the results to several analytical studies, in which the models developed in the previous chapters are used to evaluate the performance of boiling fluid solar collectors (BFSCs). First, the instantaneous efficiency model results are compared with experimental test data in an attempt to validate the model. Second, a comparison is made between the ideal and the non-ideal models to determine the difference in the calculated yearly solar fraction. Finally, several parametric studies are performed to determine the effect of collector area, condenser size, type of refrigerant, reduced water mass flow rate between the tank and heat exchanger.

4.1 Validation of Models

The models described in the previous sections were developed to study the performance of boiling collector-condenser system, and to determine their relative sensitivity to design variables and control strategies. However, before the model results can be trusted, it is necessary to validate the model with experimental test results. The collector-condenser system tested by Fanney

(12) was chosen for the comparison between experimentally and analytically determined instantaneous system efficiency. Appendix A gives the dimensions and properties of the materials used in the collector. Figure 4.1.1 shows the experimental results for the NBS test collector. The data is plotted as a function of solar radiation. The instantaneous efficiency of the test collector does not show any detectable solar radiation dependence. Figure 4.1.2 shows the instantaneous efficiency of the collector as predicted by the ideal and the non-ideal models. Two points of interest should be noticed. First the non-ideal model efficiency points lie almost on top of the ideal efficiency curve for the system tested. This indicates that the ideal model can be used in place of the non-ideal model. The second point to notice is how closely the analytically predicted results compare with the experimental data. The difference between the two is mainly due to a slight difference in the slope of the lines. If the collector loss coefficient (U_L) is adjusted, the analytical results will lie on top of the experimental data points. Since U_L was calculated analytically, it is very likely that it was slightly over estimated.

The ideal model developed in chapter 2 appears to be adequate for modeling the boiling fluid solar collector in

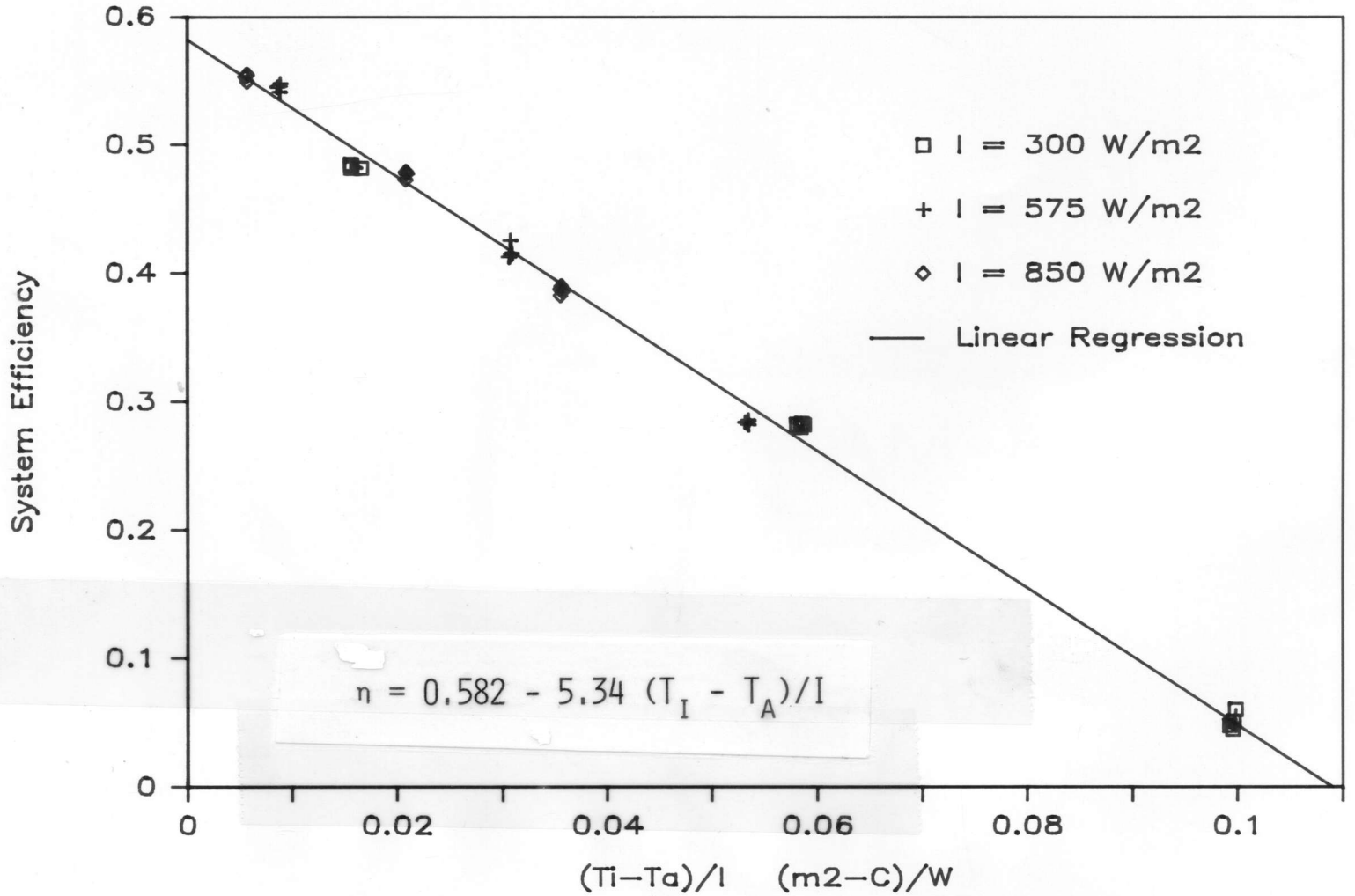

4.1.1 Instantaneous Efficiency for NBS BFSC (Experimental Test Data)

this study, for the operating conditions considered. The best method for modeling this collector is to use the $F_R(\tau\alpha)$ and $F_R\ U_L$ determined from the instantaneous collector efficiency tests and to use them in the standard Hottel-Whillier equation. The conclusions which can be drawn from the comparison of the experimental data and the model results are very limited except for the specific case tested. The results cannot be extrapolated to determine how the collector would perform at much colder ambient temperatures, or with longer or smaller diameter pipes.

A similar system was tested by Al-Tamimi (14). He performed a more in-depth study to determine the effect of subcooling on the collector's instantaneous efficiency. He accomplished this by artificially subcooling the liquid entering the collector. This is the main difference between his test of the BFSC and that of NBS. A decrease in collector efficiency and a dependence on solar radiation intensity was seen when subcooling was introduced. However, none of his data were available on which to base comparisons, but the non-ideal model does predict the same type of behavior for subcooling of the liquid entering the collector.

4.2 Long-Term Performance

A plot of instantaneous collector-condenser system efficiency is informative when comparing different collectors, but it is less useful for estimating the long-term performance of a solar domestic hot water (SDHW) system. The yearly solar fraction, the quantity of energy supplied by solar energy, is a useful measure of system performance. The SDHW system modeled in this study is described in chapter 1. The physical dimensions and parameters used in the base system studied here, are listed in Appendix A. Yearly simulations were run for boiling collector-condenser systems in several locations, to determine if the reduction in system efficiency caused by friction, hydrostatic head, and heat losses are significant. The results are listed in Table 4.1. As might be expected the yearly solar fraction varies dramatically from one location to another. The effect of hydrostatic head and friction in the vapor line has virtually no effect on solar fraction, for the system tested. As might be expected the effect of friction is most apparent in the system with the largest solar gain, Phoenix, AZ. Only pipe heat losses effect the solar fraction in an appreciable manner. Pipe losses accounted for only a 3 to 4% reduction in solar fraction from the ideal model. Note that 4 significant

Table 4.1 Simulation Results of Models and f-Chart by Location (Solar Fraction and Percent Difference from Ideal).

Location	Madison	Phoenix	Albuquerque	Seattle
Ideal Model	0.2921 ------	0.5182 ------	0.4694 ------	0.2420 ------
Hydrostatic Head Included	0.2902 0.7 %	0.5160 0.4%	0.4671 0.5 %	0.2403 0.7 %
Friction and Hydrostatic Head	0.2901 0.7 %	0.5156 0.7 %	0.4668 0.6 %	0.2401 0.8 %
Heat Losses, Friction Hydrostatic Head	0.2815 3.6 %	0.5041 2.7 %	0.4525 3.6 %	0.2338 3.4 %
f-Chart No (Pipe Losses)	0.29	0.54	0.47	0.27
f-Chart Yes (Pipe Losses)	0.29	0.53	0.46	0.26

digits were used in table 4.1 to compare the differences in the ideal and non-ideal BFSC models. This was done only o determine the magnitude of each effect. In practice only the first 2 significant digits should be used for comparisons.

The model was tested in Madison, WI, to determine it the type of refrigerant used in the collector effected the yearly solar fraction. The results show a minor improvement in solar fraction when R-12 is used in place of R-11. This is likely due to the fact that the saturation temperature of R-12 is less sensitive to pressure than R-11 (see figure 3.1.2). The gains in solar fraction, however, will probably not offset the added construction and material costs necessary to withstand the higher pressures developed by R-12.

Finally a comparison is made between f-Chart and the models developed for BFSCs. The results indicate that f-Chart can be used to predict the yearly solar fraction for and ideal BFSC. The largest deviation occurs in Seattle, WA, where f-Chart has historically over predicted the yearly solar fraction. f-Chart allows heat losses to be included in the calculation. The physical processes which result from heat losses in BFSCs are the same as those in hydronic collectors. However, heat losses can be included to more

closely approximate the solar fraction determined by the non-ideal model, which includes heat losses. The solar fraction determined by f-Chart can be assumed to be an upper bound on the solar fraction which can be obtained from a boiling fluid solar collector.

4.3 Parametric Studies

Parametric studies were performed using simulations for March in Madison, Wisconsin. The parametric studies included the effect of condenser size, UA_{cond}, and collector area, A_c, on monthly solar fraction. These studies were performed for the base case system, and for a higher quality, selective surface collector. Figure 4.3.1 shows the effect of condenser size on monthly solar fraction. The base case system condenser appears to be of more than adequate size for both collectors, as seen from the flatness of the curve for the size of the base case condenser. Figure 4.3.2 shows how the monthly solar fraction varies with collector area. This assumes a constant condenser size, but the mass flow rate of water in the condenser is proportional to the collector area (90 kg-hr-m^2). Figure 4.3.2 appears very much like the curve of solar fraction versus collector area for standard SDHW systems.

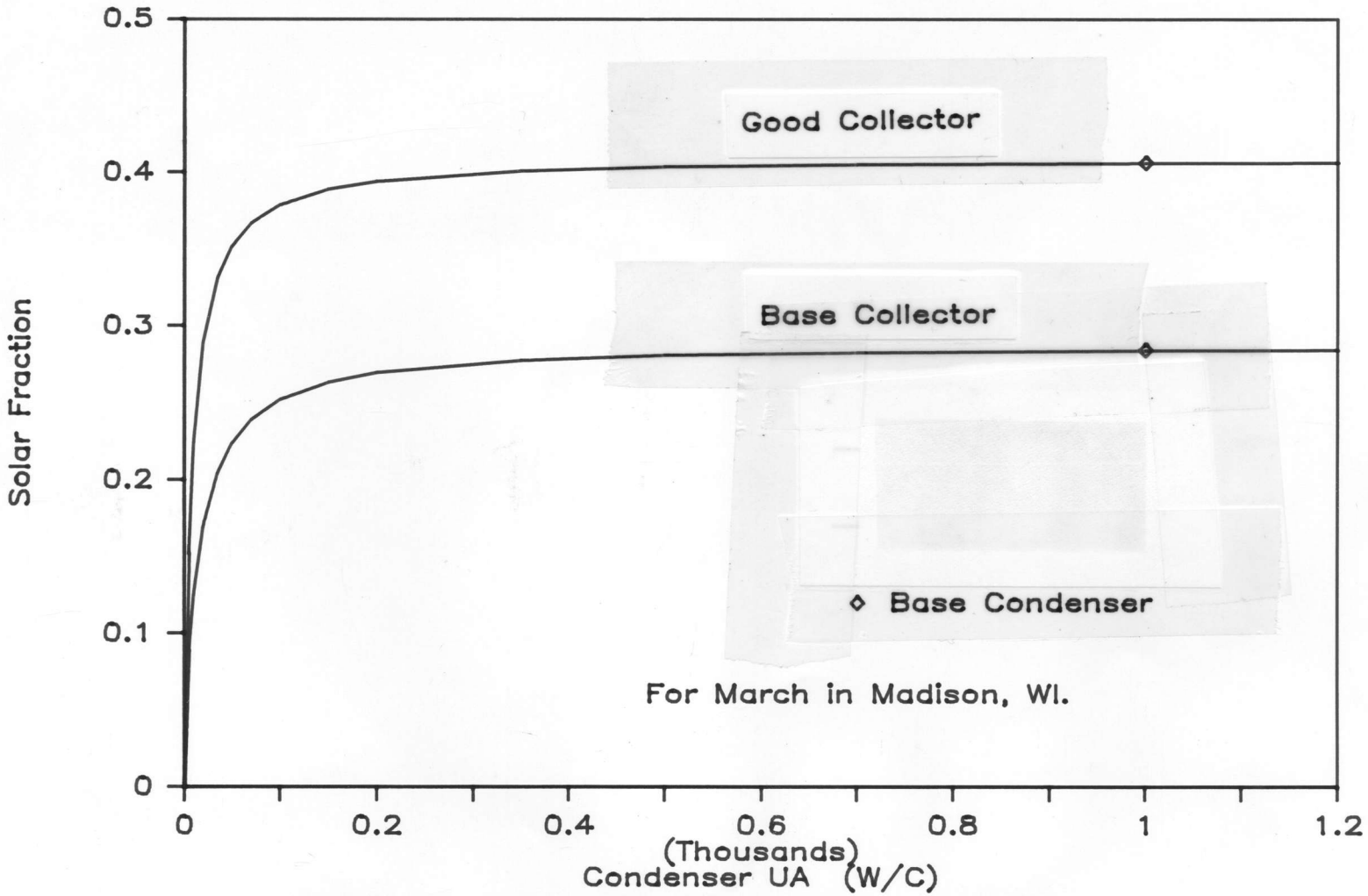

4.3.1 Effect of Condenser Size on Solar Fraction

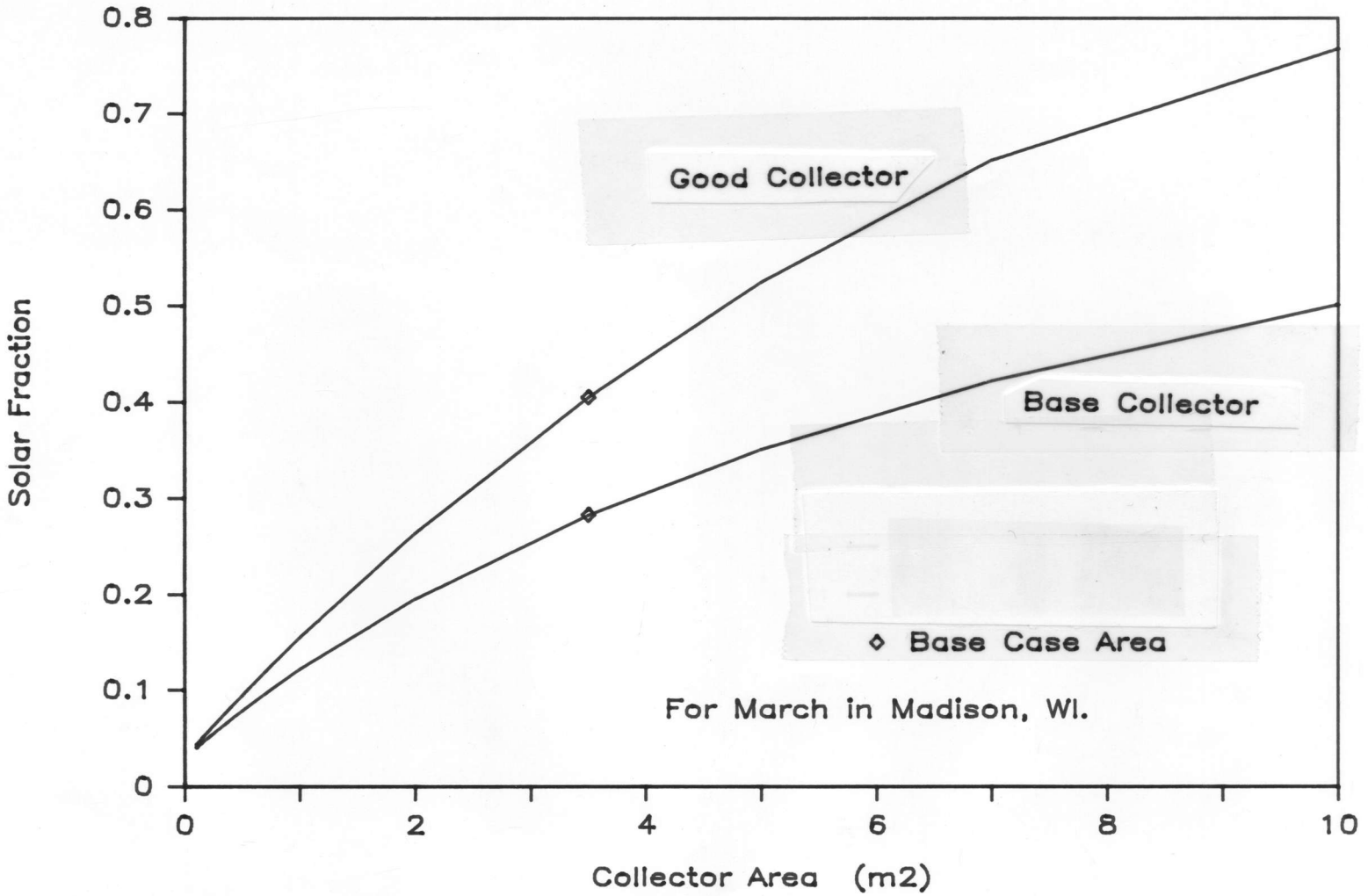

4.3.2 Effect of Collector Area on Solar Fraction

An interesting control strategy investigated by Wuestling (29) for standard hydronic solar collectors, is the reduction of the mass flow rate of water through the collector, to increase thermal stratification in the preheat storage tank. F_R is reduced by doing this, but the increased temperature stratification in the pre-heat tank lowers the average temperature of the water entering the collector and increases the average temperature of the fluid being supplied to the load. Wuestling determined that optimum system performance occurred when the average daily collector mass flow rate was approximately equal to the average daily load flow, a condition which occurs at approximately 20% of normal collector flow rates (10 l/hr-m^2). At reduced flows, annual system performance was as much as 15% higher than systems with high collector flow rates and therefore unstratified storage. Figure 4.3.3 illustrates the effect of collector mass flow rate on solar fraction for a standard hydronic SDHW system.

In systems with a heat exchanger located between the collector and pre-heat storage tank, it is not the mass flow rate in the collector but rather the tank-heat exchanger flow which must be reduced to reduce recirculation of water in the storage tank. However, the effectiveness of the heat exchanger will be reduced if the mass flow rate of the tank-

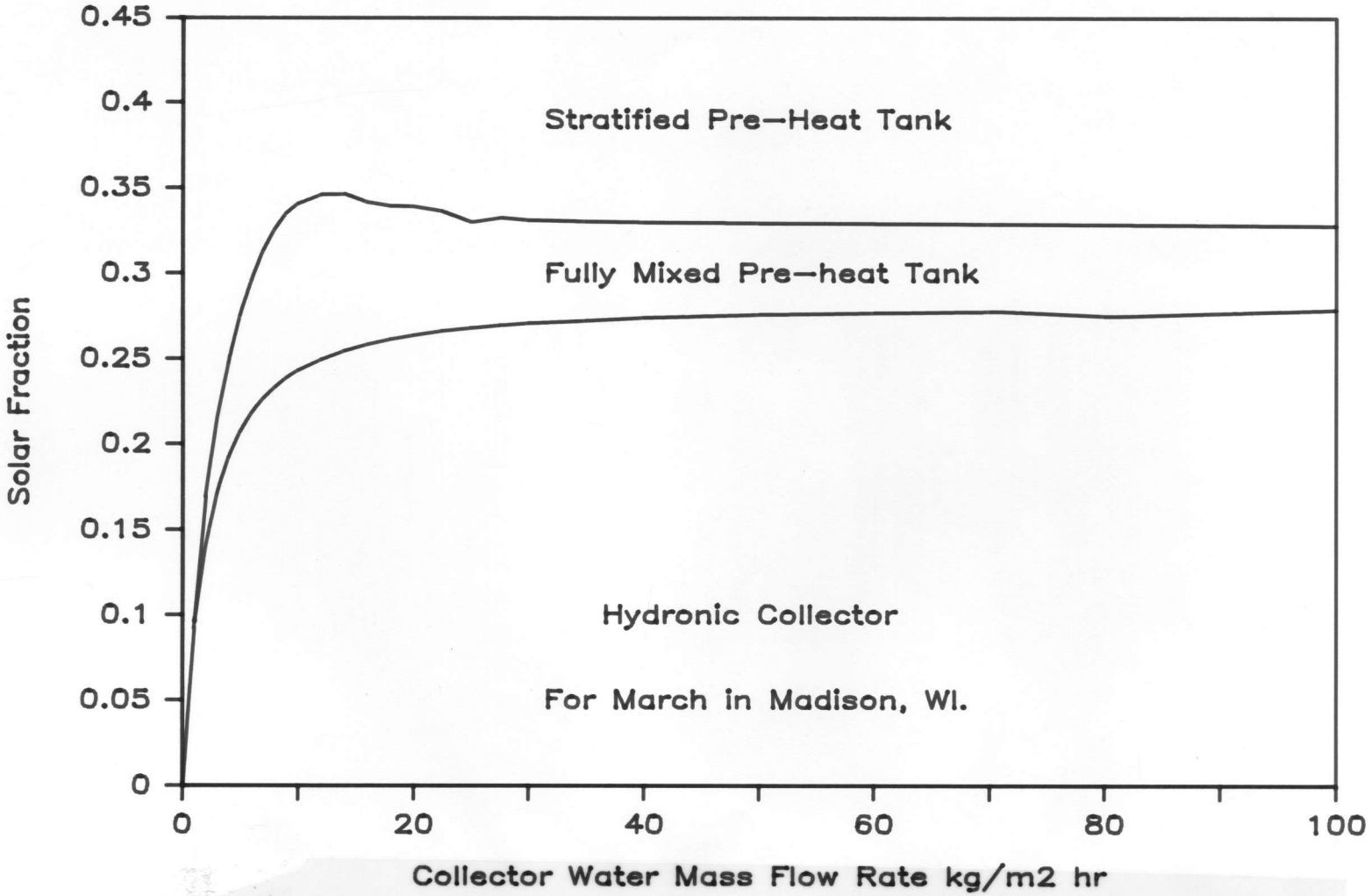

4.3.3 Effect of Reduced Collector Water Flow Rate on Solar Fraction for a Hydronic Collector

heat exchanger flow is reduced. The trade off in the boiling collector SDHW system to obtain a stratified preheat storage tank is a reduction in condenser UA, and therefore in F_R'.

The effect of condenser water flow rate was examined by simulations in the Madison climate for both fully-mixed and stratified preheat storage tanks. Figure 4.3.4 shows the solar fraction as a function of condenser water mass flow rate for the fully-mixed and stratified cases. The results for the fully-mixed tank show an increasing but asymptotic dependence of monthly solar fraction on flow rate, as in the case for hydronic collector. At low mass flow rates the boiling collector system does not perform as well as the hydronic case, because the condenser UA is penalized more at low flow rates than collector F_R. The boiling collector with a fully mixed pre-heat tank performs better than the fully mixed boiling collector, but shows an optimum flow rate. The optimum for the base case system occurs at a higher flow rate than a comparable hydronic system because the gain in condenser UA at higher mass flow rates offsets the gain due to stratification in the tank at low mass flow rates. The optimum also is not as pronounced as in the hydronic case. Figure 4.3.5 shows how the optimum flow rate for the stratified case varies through out the year in

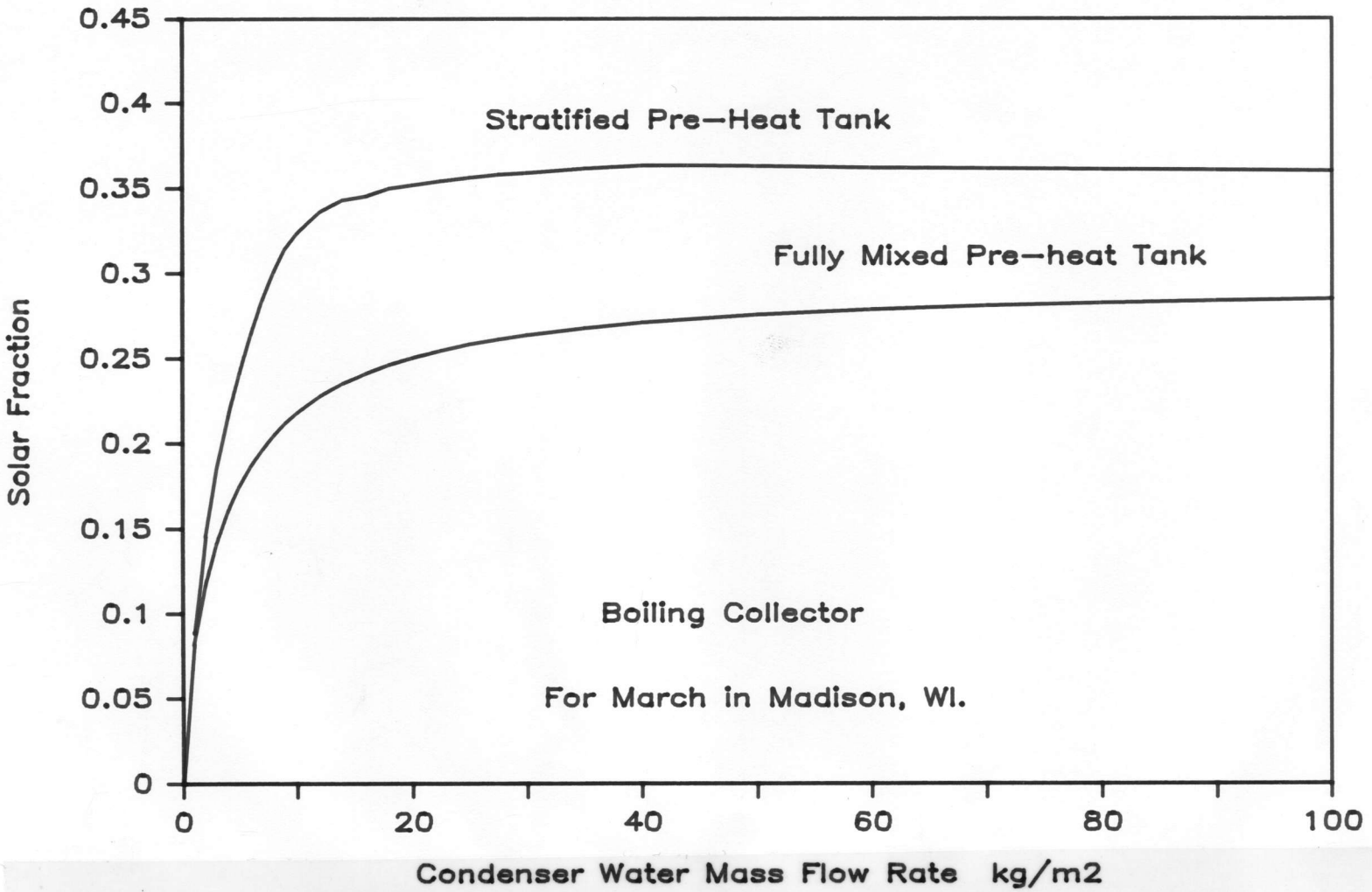

4.3.4 Effect of Reduced Condenser Water Flow Rate on Solar Fraction for a BFSC

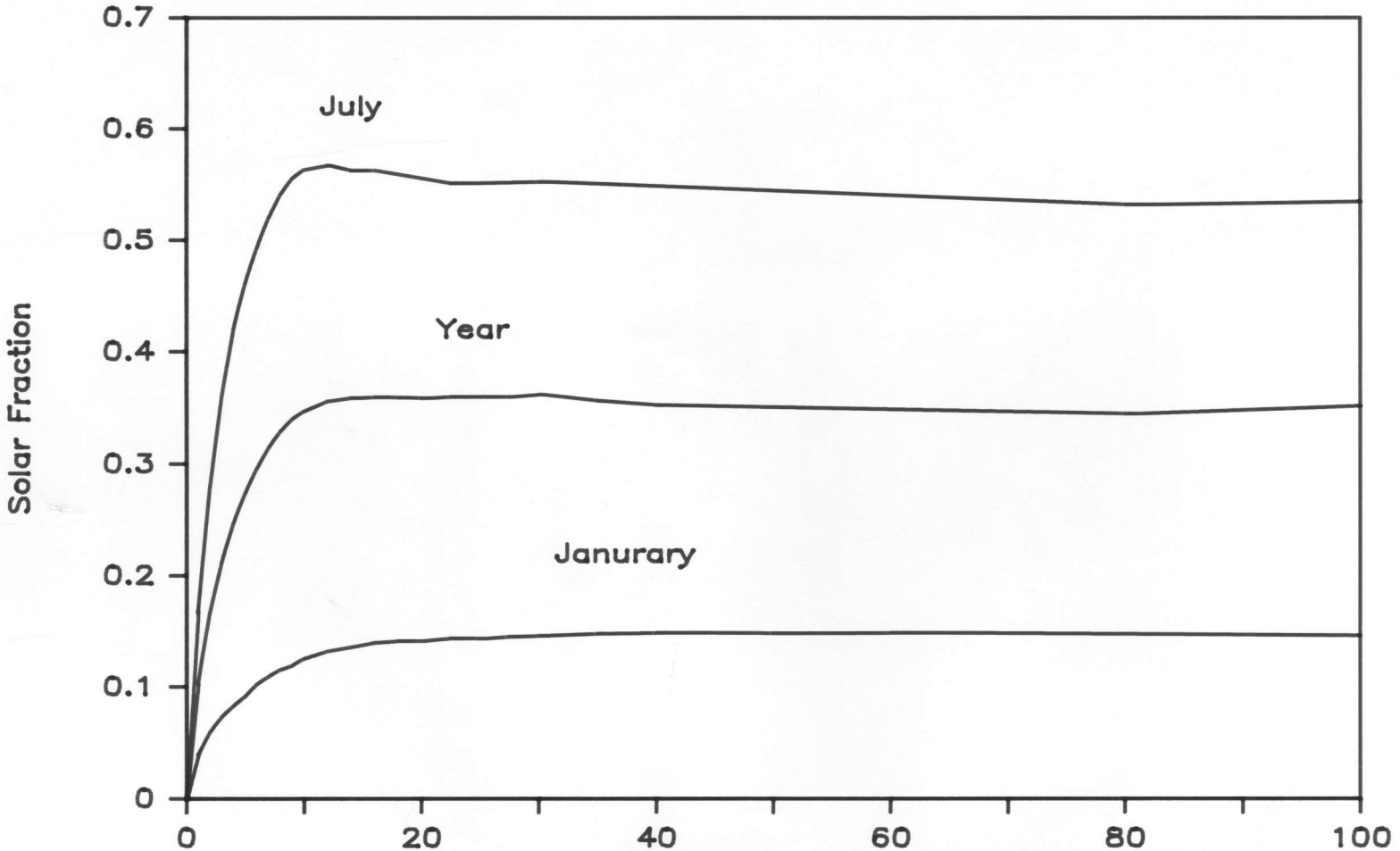

4.3.5 Monthly Variation in Solar Fraction for Reduced Water Flow Rates in BFSCs

Madison, Wisconsin. During warmer months the optimum flow rate is lower than for cold months. Increased collector losses offset the gains due to increased stratification in the pre-heat storage tank. Figure 4.3.6 illustrates the same effect of stratification in pre-heat tank for several locations around the country, for the month of July. The optimum solar fraction occurs at almost the same mass flow rate for all locations (10 to 15 kg/hr m2).

4.4 Summary

This chapter applies the ideal and the non-ideal boiling fluid collector models developed in the previous chapters. Experimental data is used to validate the results of the models. The model predictions correspond very well with the experimental results. However, the data available only covers a small range of operating conditions, and thus limits the range over which the models can be used reliably. Yearly solar fractions of the base case system are determined for several locations. A comparison is made at each location to determine the effect of friction, hydrostatic head , heat losses and type of refrigerant on yearly solar fraction. For the system tested only heat losses effect the yearly solar fraction in an appreciable manner. f-Chart was found to agree with the results of the ideal BFSC model. f-Chart can be used to predict an upper

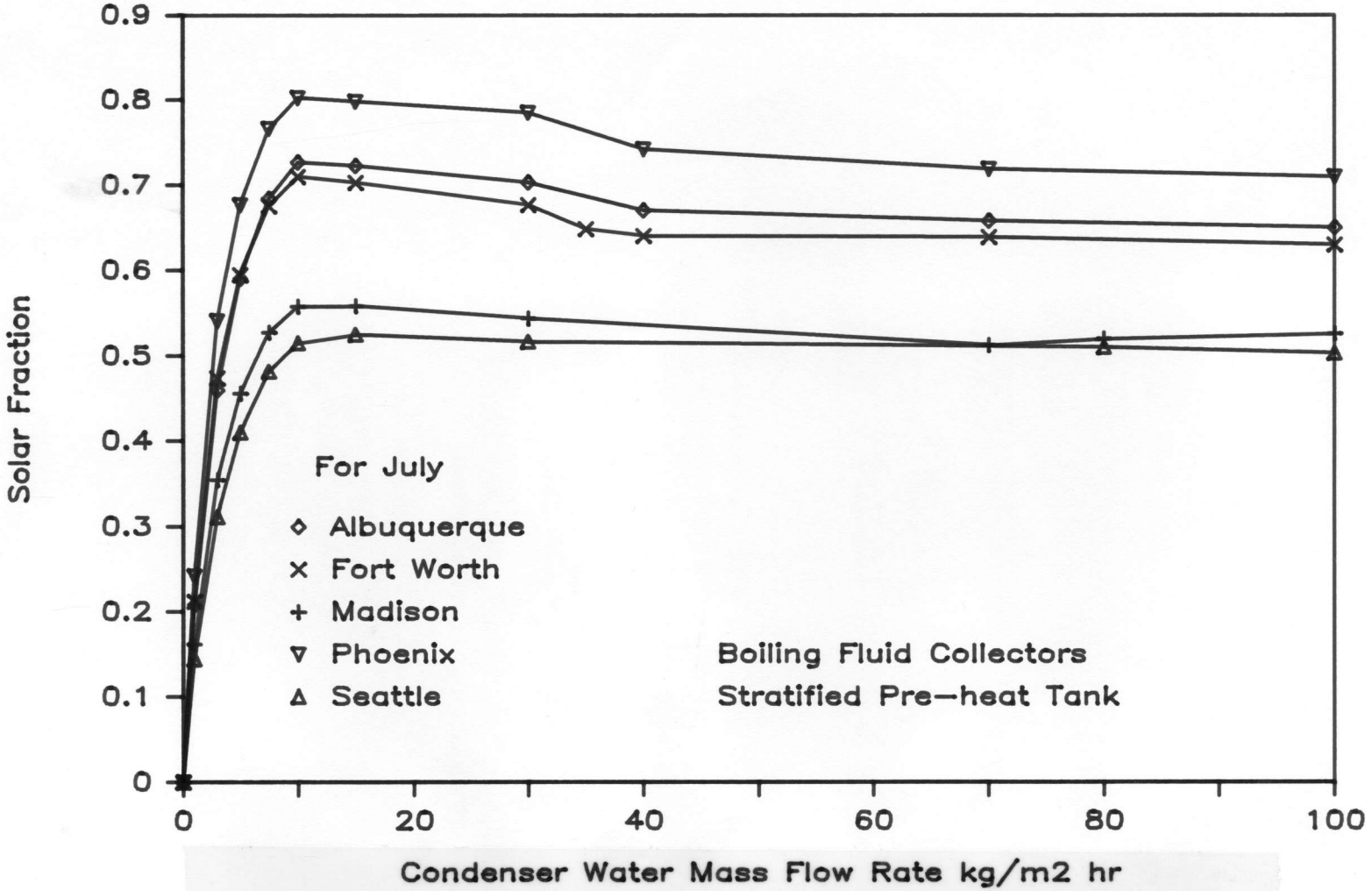

4.3.6 Effect of Location on Solar Fraction for Reduced Water Flow Rates in BFSCs

bound for the yearly solar fraction of BFSC systems. Several parametric studies are performed to determine the effect of condenser UA, collector area, and stratification in the pre-heat storage tank on solar fraction.

5. Analytical Models of Boiling Fluid Flow

Up until now, the boiling fluid solar collector has been considered to be a "black box." In order to fully understand the operation of boiling fluid solar collectors it is necessary to model the boiling section of the collector accurately. The basic fluid regimes and temperature profiles which occur in the boiling fluid collector were discussed in chapter 3. No indication was given at that point how or why these changes occurred or how they could be predicted. To do this it is necessary to analyze the physical processes which occurin boiling fluid flow. In this chapter three models are considered to study the fluid dynamics of two-phase flow.

5.1 Introduction

The analysis of a single-phase flow is simplified if it can be determined whether the flow is laminar or turbulent. Likewise it is helpful to know this kind of information when analyzing two-phase flow. When a liquid is vaporized in a heated channel, a variety of liquid-vapor flow patterns are created. The particular flow pattern depends on conditions such as heat flux, flow, pressure, and channel geometry. The presence of a heat flux alters the flow patterns which

might have occurred in a long unheated channel at the same flow conditions.

The typical procession of flow patterns in an inclined boiling fluid solar collector are likely to be: subcooled liquid, bubbly flow, slug flow, annular flow, drop flow and superheated vapor. These flow patterns are illustrated in figure 5.1.1. Subcooled liquid and superheated vapor have been previously discussed in chapter 3.

Bubbly flow occurs when the vapor generated in the collector is distributed as discrete bubbles in a continuous liquid phase. At one extreme bubbles may be small and spherical and at the other extreme the bubbles may be large with a hemispherical cap and a flat tail, but still much smaller than the pipe diameter. During bubbly flow the individual vapor bubbles will collide and coalesce to form larger bubbles. A useful property for determining the state of a two-phase flow is the void fraction, α. The void fraction is the ratio of gas phase flow area to total flow area.

$$\alpha = A_g/A \qquad (5.1.1)$$

Bubbly flow usually exists for void fractions less than 0.3.

In slug flow the vapor bubbles are approximately the diameter of the pipe. The bubble has the characteristic

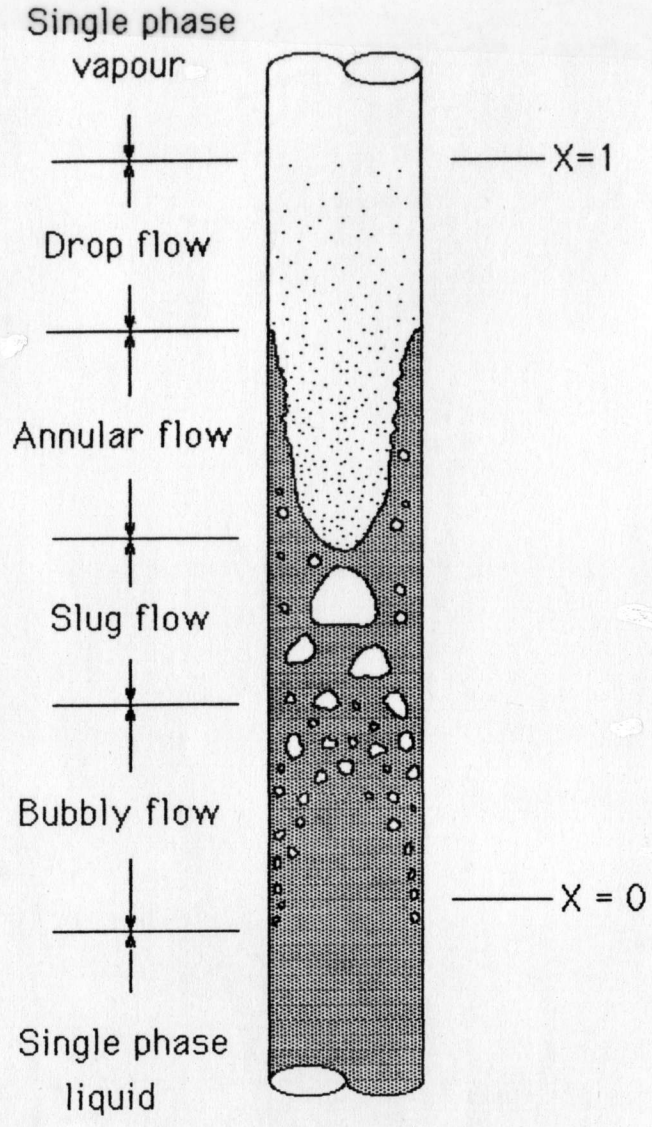

Figure 5.1.1 Flow Patterns in a Boiling Fluid Solar Collector

hemispherical cap and the vapor is separated from the wall by a descending film of liquid. The upward liquid flow is in slugs of liquid trapped between successive vapor bubbles. Slug flow is usually associated with void fractions up to 0.8.

A thin liquid film forms at the pipe wall during annular flow with a continuous central vapor core. Waves are usually present on the surface of the liquid film. These waves continually break up to form droplets that are entrained in the central vapor core.

Drop flow occurs only in heated channels. Drop flow begins when the last liquid at the pipe wall is vaporized. This is due to the radial temperature profile in the channel. Any liquid at the wall has already been vaporized, and only the liquid mist at the center of the tub remains to be vaporized. Droplets may exist even though vapor along the pipe wall is superheated.

If the change in quality over the change in length is large then the development of each flow pattern is disrupted. Some flow patterns will be expanded others compressed, and some may even disappear. Slug flow, for example, may be absent in short channels.

Three techniques are considered in this chapter for modeling the fluid dynamics of the two-phase region in a

boiling fluid collector. These are: model the two-phase region as if it were a liquid, use the homogeneous model, and the separated flow-drift flux model. The next section discusses the methods of analysis used in each of these models.

5.2 Methods of Analysis

The technique used to analyze two-phase flow are extensions of the methods already used for single phase flow. The general approach is to write down the basic equations for a two phase mixture. Collier (25) develops the basic equations of conservation of mass, momentum and energy for a one-dimensional analysis of boiling flow. However to solve these equations it is necessary to make assumptions about the velocity of each phase, the area occupied by each phase, friction between the phases and friction between the fluid and the wall. Each of the models developed below makes specific assumptions as to the nature of the two-phase flow. The assumptions made by any one model may or may not be appropriate for the application of boiling fluid solar collectors.

Single-Phase Liquid Model

The single-phase liquid model considers the collector to be a big boiling pot of liquid, where the formation of vapor has very little effect on the density of the liquid.

This model is very simplistic and is the basic approach taken in chapter 3. The model works adequately for determining the energy gained by the collector for some situations, but it gives us no information about the phenomena occurring in the collector. The two following models were introduced to help understand the physical processes in the collector.

The Homogeneous Model

The homogeneous model is a second method which can be used to model two-phase flow in boiling fluid solar collectors. The homogeneous model considers the liquid and vapor to flow as a single phase with average fluid properties. The three basic assumptions of the homogeneous model are: equal vapor and liquid velocities, thermodynamic equilibrium between phases, and a single-phase friction factor defined for two-phase flow.

Collier (25) develops the basic equation for evaluating the pressure drop in boiling homogeneous flow. For the case where liquid is evaporated from a saturated inlet condition to a vapor quality X, and the compressibility for the gas phase can be neglected and (ν_{fg}/ν_f), the friction factor f_{TP}, and the change in X are constant over the length L_b, then the pressure drop can be expressed as:

$$\Delta P = \frac{2\, f_{TP}\, L\, G^2\, \nu_f}{D}\left[1 + \frac{X}{2}\left(\frac{\nu_{fg}}{\nu_f}\right)\right] + G^2\, \nu_f \left(\frac{\nu_{fg}}{\nu_f}\right) X \qquad (5.2.1)$$

$$+ \frac{g \sin\beta\, L}{\nu_{fg}\, \bar{X}} \ln\left[1 + X\left(\frac{\nu_{fg}}{\nu_f}\right)\right]$$

The two-phase fanning friction factor is found using:

$$f_{TP} = .079 \left(\frac{G\, D}{\bar{\mu}}\right)^{-1/4} \qquad (5.2.2)$$

The mean two-phase viscosity $\bar{\mu}$ is found using a relationship developed by McAdams (30).

$$\bar{\mu} = X\, \mu_g + (1 - X)\, \mu_f \qquad (5.2.3)$$

Separated Flow - Drift Flux Model

Unlike the homogeneous flow model which assumes the vapor and liquid form a single "pseudo phase," the separated flow model separates the vapor and liquid into two streams. The basic assumptions of the separated flow model are: constant vapor and liquid phase velocities, thermodynamic equilibrium between phases, and an empirical relationship to relate the two-phase friction multiplier (ϕ^2) and the void fraction (α) to the independent flow variables.

The separated flow model can be used to evaluate the pressure drop in a boiling fluid solar collector. The pressure drop can be determined analytically assuming that the compressibility of the gas phase can be neglected and that the specific volumes (ν_g and ν_f) and the friction factor f_{fo} are constant over the length considered. If a saturated liquid enters, the change in quality is linear and a mixture of quality X leave, then the pressure drop is:

$$\Delta P = \frac{2 f_{fo} G^2 \nu_f L}{D}\left[\frac{1}{X}\int_0^X \phi_{fo}^2 \, dx\right] + G^2 \nu_f \left[\frac{X^2}{\alpha}\frac{\nu_g}{\nu_f} + \frac{(1 - X)^2}{(1 - \alpha)^2} - 1\right] + \frac{L g \sin\beta}{X}\int_0^X \left[\rho_g \alpha + \rho_f (1 - \alpha)\right] dx \qquad (5.2.4)$$

The two-phase multiplier (ϕ_{fo}^2) is evaluated using:

$$\phi_{fo}^2 = \phi_f^2 (1 - X)^{1.75} \qquad (5.2.5)$$

Where ϕ_f^2 is calculated using:

$$\phi_f^2 = (1 - \alpha)^{-2} \qquad (5.2.6)$$

The drift-flux model is used to determine the void fraction in the boiling fluid collector. Drift-flux theory is useful

for analyzing flow regimes in which gravity is balanced by the pressure gradient and forces between components. The drift-flux is the volumetric rate at which vapor is passing upward greater than the average volumetric rate of the fluid. Thus, it is a function of the relative velocity between phases. The average void fraction in the collector according to the drift flux model is:

$$\bar{\alpha} = \frac{\bar{\beta}}{C_o + \frac{\bar{u}_{gj}}{(\bar{j})}} \tag{5.2.7}$$

The mean drift velocity ($\bar{u}_{gj}$) is dependent on the flow pattern. In this analysis, the flow pattern in the collector is assumed to be bubbly-slug flow. For bubbly-slug flow, $\bar{u}_{gj}$ is found using:

$$\bar{u}_{gj} = .56 \left[\frac{g\,(\rho_f - \rho_g)\,D}{\rho_f} \right]^{1/2} \tag{5.2.8}$$

The average volumetric flux, $\bar{j}$, and the volumetric quality, β, are found using the following:

$$\bar{j} = \frac{\bar{Q}}{A} \tag{5.2.9}$$

$$\bar{\beta} = \frac{\bar{Q}_g}{\bar{Q}_g + \bar{Q}_f} \tag{5.2.10}$$

5.3 Results

All three models developed in the previous section have been used to evaluate the pressure drop in the boiling section of the collector. The results shown in chapters 3 and 4 use the first method. The homogeneous model and the separated flow - drift flux model were also used to study the fluid dynamics in boiling fluid collectors. Several other investigators have used the homogeneous model to model boiling fluid solar collectors (14,17), however there in nothing in the literature showing the drift-flux model being applied to this application.

The models developed in this chapter are difficult at best to verify. Thus in order to feel confident in what they tell us, they should agree with observed or known behavior. For example, the initial mass of refrigerant in the system is known. At any point in time, the total mass in the system is a constant. A second fact is that the sum of the pressure drop (or increases) around the refrigerant loop is zero. And finally, the physical dimensions limit the hydrostatic head of liquid that can over come friction in the system. The actual operating condition in the collector must adjust such that all of these are true.

When the homogeneous model was first used, it was assumed that the mass flow rate of the refrigerant in the collector was the same as the mass flow rate of vapor going to the condenser. Thus, all of the refrigerant in the collector is vaporized by the time it reaches the top of the collector. However, when this was simulated using the homogeneous model, a mass balance indicated that the initial fill of liquid refrigerant in the collector was only about 5% of the collector. In practice these types of collectors are filled 70 to 90% with liquid refrigerant. Thus the quality at the top of the collector must be less than 1.0.

The boiling collector tested has a liquid-vapor separator built into it. It is likely that some liquid is entrained in the vapor and is returned to the bottom of the collector, allowing only the vapor to continue on to the condenser. Using the same approach as above, it is also possible to determine what exiting quality is necessary for each energy input to give the correct initial fill of liquid refrigerant in the collector. Using a homogeneous model Al-Tamimi (14) predicted exiting qualities of 40 to 80% for R-11 in the same type of collector. Abramzon et al. predicted exiting qualities around 5 and 15% for acetone and R-113, in a thermosyphoning flat-plate collector. The homogeneous model used in this study predicted exiting

qualities of approximately 1% for R-11, for an initial fill of 70%. However, this causes a large reflux of liquid and a large pressure drop across the collector. The pressure drop is not realistic since it requires a hydrostatic head of liquid greater than the height of the collector, which is the maximum possible if the liquid-vapor separator in included in the collector.

The drift-flux model was also used to predict the exiting quality in the collector. The predicted exiting quality for the drift-flux model ranged between 5 and 10%. This range of exiting quality is more reasonable than the 1% predicted be the homogeneous model. However, the pressure drop in the collector was still fairly large, but not as large as in the homogeneous case.

It is difficult to believe that the correct state in the collector was determined by either model. Very little experimental work has been done on this type of boiling to determine the actual boiling flow patterns which develop. However, the drift-flux model should be more appropriate for modeling gravity induced flow than the homogeneous model.

5.4 Summary

This chapter took a more detailed look at the actual fluid conditions which exist in a boiling fluid solar collector. Three methods of modeling the two-phase region

of the collector were considered. Of these the drift-flux approach seems most appropriate. However, more information is needed about the actual processes occurring in the boiling collector to do a adequate job modeling the two-phase flow.

6. Conclusions and Recommendations

A detailed Boiling Fluid Solar Collector (BFSC) model was developed for use with TRNSYS, capable of modeling a wide range of BFSC types. This model accounts for a subcooled liquid entering the collector, dryout and superheating of the vapor, heat losses in the vapor and liquid return lines, pressure drops due to friction in the collector and piping, and the effect of fluid hydrostatic head.

The effect of friction in the collector, vapor and liquid return line can be a very important factor in determining the performance of a BFSC system. Frictional pressure drops are responsible for both subcooling and superheating in the collector. Subcooled and superheated states in the collector cause the solar radiation dependence on the instantaneous collector efficiency, as reported by others (14,17).

For and ideal boiling fluid flat-plate collector-condenser system, for which a saturated liquid enters the collector, and a saturated vapor exits, the efficiency curve has the same form as that of conventional non-boiling

flat-plate collectors. The boiling flat-plate collector-condenser system tested by Fanney (12) exhibits this form. It appears that careful design can reduce the amount of subcooling and superheating to a point that they have a negligible effect on collector performance. In many boiling flat-plate collector systems where heat losses and the effects of friction are minimal, a simplified approach can be used to model the system performance. A modified form of the the collector heat removal factor, F_R', is used to account for the effect of the condenser. The f-Chart method (29) can then be used to predict the long-term performance of the boiling collector system. The assumptions made using this simplified approach are optimistic and yield a maximum performance estimate. However, studies done with the more detailed model show that the sensitivity of long-term performance to subcooling and moderate pressure losses is small.

The new ASHRAE 109 testing procedure has been developed for BFSCs. Although a special procedure is needed for BFSCs, the new test does not sufficiently improve on the Standard 93-77 test to make it useful. The results of the ASHRAE 109 test alone cannot be used by themselves to determine the instantaneous thermal performance of a BFSC. Thus, f-Chart and other design

procedures cannot be used to determine long-term performance. In many cases, the required subcooling test cannot be performed because the condenser is located inside the collector box. A better test procedure is needed to adequately determine the performance of BFSCs, and still be flexible enough to handle many collector-condenser configurations. However, for well designed systems where friction and heat losses are negligible, the 93-77 test can be used with good results.

A limiting factor on this research has been the limited amount of experimental data available. More detailed experimental research is needed. Specifically, a detailed study of two-phase flow in BFSCs, and the development of a boiling flow model to predict pressure drops and the void fractions in the collector. Three approaches were taken for modeling the two-phase fluid flow in this research. The Drift-flux separated flow model was found to be the most appropriate model for gravity induced boiling flow as compared with the homogeneous model which has been used by most investigators in the past. Also more experimental tests are needed to determine the effects of heat losses from the refrigerant lines, and pressure drops in the collector and refrigerant lines.

APPENDIX A

COLLECTOR AND SYSTEM PARAMETERS

COLLECTOR

Gross Area	4.08 m2
Net Area	3.51 m2
Absorber Plate	Steel 1.8 m long 1.94 m wide 1.76 mm thick ε = .75 α = .91
Risers	Steel 32 flow tube 9.53 mm OD 7.77 mm ID
Cover Plates	2, Tedlar .1 mm thick τ = .93 Index of Refraction = 1.45 15.9 mm space between covers 63.5 mm space between plate & cover
Insulation	Glass Fiber back 63.5 mm edge 25.4 mm

SYSTEM PARAMETERS

COLLECTOR	BASE	HIGH QUALITY
AREA	4.08m	4.08m
F'b	0.96	0.96
F'	0.56	0.56
UL	7.5 W/m2 C	3.6 W/m2 C
($\tau\alpha$)	0.676	0.80

PREHEAT TANK	
Volume	303 liters
Thermal Conductance	1.081 W/m2 C
Envelope Temperature	21 C

AUXILIARY TANK	
Volume	151 liters
Thermal Conductance	1.047 W/m2 C
Envelope Temperature	21 C
Set Temperature	60 C
RAND Load Profile	300 liters/day

CONNECTING LINES	VAPOR	LIQUID
Diameter	0.0141 m	0.0141 m
Length	10.0 m	10.0 m
UA	2.5 W/m2 C	5.0 W/m2 C

APPENDIX B

SAMPLE TRNSYS SIMULATION DECK

This appendix contains a listing of one of the TRNSYS simulation decks used in this research. This uses the boiling fluid collector-condenser model and a fully mixed solar preheat storage tank. This is the same system shown in figure 1.2.1.

```
CONSTANTS 28
BEG=1    END=8760
N=2    FB=.96    FL=.55    UL=27.    AC=3.51
AG=AC * 1.16    NST=1    REF=1     LAT=43.1
B=LAT    LOAD=300.    HSH=1.8    VD=.0141
VL=10    TA=21.0    TM=10.4    TSET=60.0
XMC=50   CPW=4.190    PF=1000.    DTDB=10    HX=1
UA=3600 * HX    XM=XMC * AC   UAL=5.0    UAV=2.5
************************************************
*                                              *
*           BOILING COLLECTOR                  *
*                                              *
************************************************
WIDTH 80
SIMULATION BEG END 1.0
TOL -.01 -.01
LIMITS 50 60 50
NOLIST
*
UNIT 9 TYPE 9 TMY DATA READER
PARAMETERS 7
2 1 -1 1 0 -1 1
(24X,F4.0,F5.1)
*
UNIT 16 TYPE 16 RADIATION PROCESSOR
PARAMETERS 7
3 1 NST LAT 4871. 0  -1
INPUTS 6
9,1 9,19 9,20 0,0 0,0 0,0
0 0 0  .2 LAT 0.0
UNIT 2 TYPE 2  DIFFERENTIAL CONTROLLER
PARAMETER 3
5 1 25
INPUTS 3
1,1    5,1    2,1
TM     TM     0
UNIT 3 TYPE 3 PUMP
PARAMETER 1
XM
INPUTS 3
5,1    5,2    2,1
TM     0      0
UNIT 1 TYPE 37 BOILING SOLAR COLLECTOR
PARAMETERS 20
1 AG AC FB FL .91 N UL .03 1.45 B
UA REF CPW VL VD HSH HX UAL UAV
INPUTS 6
3,1 3,2 9,2 16,6 16,9 1,4
TM    0    20   0     0     -1
UNIT 14 TYPE 14 LOAD
```

```
PARAMETERS 82
0,0 5,0 5,.125 6,.125 6,.391 7,.391 7,.625 8,.625
8,.703 9,.703 9,.549 10,.549 10,.391 11,.391
11,.297 12,.297 12,.422 13,.422 13,.242 14,.242
14,.203 15,.203 15,.156 16,.156 16,.297 17,.297
17,.549 18,.549 18,1.0 19,1.0 19,.786 20,.786
20,.549 21,.549 21,.422 22,.422 22,.391 23,.391
23,.156 24,.156 24,0
UNIT 15 TYPE 15 CALC.  LOAD MASS FLOW
PAR 6
0 0 2 0 1 -4
INPUTS 3
0,0 0,0 14,1
LOAD 8.254 0.0
UNIT 5 TYPE 4 PREHEAT STORAGE TANK
PAR 6
1 .303 CPW PF 3.9 -.8
INPUTS 5
1,1 1,2 11,1 11,2 0,0
TM 0 TM 0 TA
DERIVATIVES 1
TM
UNIT 4 TYPE 4     AUX TANK
PAR 13
1 .151 CPW PF 3.8 -.4 32400 1 1 TSET .001 0 0
INPUTS 5
0,0 0,0 5,3 5,4 0,0
0 0 TM 0 TA
DERIVATIVES 1
TSET
UNIT 11 TYPE 11        DIVERTER (TEMP CONTR.)
PARAMETERS 2
4 8
INPUTS 4
0,0 15,1 4,3 0,0
TM 0 TSET TSET
UNIT 12 TYPE 11    TEE PIECE
PARAMETERS 1
1
INPUTS 4
4,3 4,4 11,3 11,4
TM 0 TSET 0
UNIT 28 TYPE 28 SIMULATION SUMMARY
PARAMETERS 20
-1 BEG END 13 2 -1 XMC -4 -1 AC -4 -1
HX -4 0 0 -11 3 2 -4
INPUTS 2
5,6 4,8
LABELS 4
XMC AC HX FSOLAR
```

```
UNIT 27 TYPE 27     HISTOGRAM PLOTTER
PARAMETERS 15
1 -12 -12 BEG END 0 .2 20 0 20 20 20 40 20 14
INPUT 3
1,13  1,8 1,8
0  0  0
END
```

APPENDIX C

BOILING FLUID SOLAR COLLECTOR COMPONENT MODEL

This subroutine models a boiling fluid flat-plate solar collector-condenser system.

PARAMETERS

1	MODE = 0	Ideal boiling fluid solar collector.
	= 1	Non-ideal boiling fluid collector with heat losses, friction and hydrostatic head.
	= 2	Same as 2, but calculates UA for the condenser.
2	Ag	Gross collector area (m2).
3	Ac	Net collector area (m2).
4	Fb	Boiling collector efficiency factor.
5	Fl	Non-boiling collector efficiency factor.
6	ALPHA	Collector plate absorptance.
7	N	Number of covers.
8	UL	Collector loss coefficient (kJ/m2 C).
9	XKL	Cover KL product.
10	REFRIN	Index of refraction.
11	B	Collector slope (deg).
12	UA	Condenser UA (W/m2 C).
13	Refrigerant = 1	R-11
	= 2	R-12
14	Cp	Specific heat of water (kJ/kg C).
15	VD	Vapor line diameter (m).
16	VL	Vapor line length (m).
17	HEIGHT	Length of collector (m).
18	FRACT	Fraction of Condenser Used.
19	UAL	Conductance of liquid line (kJ/C).
20	UAV	Conductance of vapor line (kJ/C).

INPUTS

1	Ti	Condenser water inlet temperature (C).
2	XMc	Condenser water mass flow rate (kg/hr).
3	Ta	Ambient Temperature (C).
4	XIT	Instantaneous solar on tilted surface (kJ/m2).
5	THETA	Angle of incidence.
6	RHOD	Reflection of N covers, initially set to -1.

OUTPUTS

1	Tcout	Condenser outlet water temperature (C).
2	XMC	Condenser water mass flow rate (kg/hr).
3	Ti	Condenser inlet water temperature (C).
4	RHOD	Connect to input 6.
5	Xmrll	Mass flow rate of refrigerant (kg/hr).
6	T	Saturation temperature at top of collector (C).
7	THX	Condenser saturation temperature (C).
8	dTsc	Number of degrees of subcooling (C).
9	Qu	Useful energy gain (kJ).
10	XIT	Instantaneous solar on tilted surface (kJ/m2).
11	XX	X coordinate for efficiency (m2 C/W).
12	EFFIC	Collector efficiency.
13	Z	Fraction of collector subcooled.
14	TAUALF	Transmittance - absorptance product.

```
C               12-15-84
C
C         THIS SUBROUTINE SIMULATES A
C BOILING FLUID SOLAR COLLECTOR AND CONDENSER
C
      SUBROUTINE TYPE37(TIME,XIN,OUT,T,DTDT,PAR,INFO)
      DIMENSION XIN(15),OUT(20),INFO(10),PAR(20)
      COMMON /DELQA/Ac,FB,XIT,TAUALF,UL,Ta,Ti,XMc,
     *              Cp,Tcout,UA
      COMMON FRACT,UA0
      REAL R(2)
      REAL Tf,pf,pg,nf,ng,kf,kg,CpR11,Cpg,hfg,REF
      DATA R/.0592,.0688/
C
C CALL SUBROUTINE TYPECK TO CHECK INPUTS
C
      IF(INFO(7).EQ.-1)THEN
      IOPT=1
      NI=6
      NP=20
      ND=0
      CALL TYPECK(IOPT,INFO,NI,NP,ND)
      ENDIF
C
C ASSIGNING OF VARIABLES
C
      MODE=PAR(1)
      Ag=PAR(2)
      Ac=PAR(3)
      FB=PAR(4)
      FL=PAR(5)
      ALPHA=PAR(6)
      N=PAR(7)
      UL=PAR(8)
      XKL=PAR(9)
      REFRIN=PAR(10)
      B=PAR(11)
      UA=PAR(12)
      UA0=PAR(12)
      REF=PAR(13)
      Cp=PAR(14)
      VD=PAR(15)
      VL=PAR(16)
      HEIGHT=PAR(17)
      FRACT=PAR(18)
      UAL=PAR(19)
      UAV=PAR(20)
      Ti=XIN(1)
      XMc=XIN(2)
      Ta=XIN(3)
```

```
      XIT=XIN(4)
      THETA=XIN(5)
      RHOD=XIN(6)
C
C SUBROUTINE TALF CALCULATES THE TAU ALPHA PRODUCT
C
      TAUALF= TALF(N,THETA,XKL,REFRIN,ALPHA,RHOD)
      S=XIT*TAUALF
      g=9.81
C
C CHECK PUMP FOR NO FLOW SITUATION
C
      IF(XMC.EQ.0.0) THEN
         TCOUT=S/UL+TA
         QU=0
         Z=1.0
         DTSC=999.
         GOTO 88
      ENDIF
C
C INITIAL GUESS     QU
C
      NCOUNT=0
      E=1-exp(-UA/(Cp*XMc))
      Frb=Fb/(1+(Ac*Fb*UL/(XMc*Cp*E)))
      Q=AC*Frb*(S-UL*(TI-TA))
      T=(s-Q/(Ac*Fb))/UL+Ta
      CALL PSAT(REF,TI,PIN)
      VA=3.142*(VD/2)**2
50    NCOUNT=NCOUNT+1
      DUMNUM=0
      Z=0.0
      Z0=0
55    DUMNUM=DUMNUM+1
      CALL SATVAL(T,pf,pg,nf,ng,kf,kg,CpR11,Cpg,hfg,REF)
      XMR11=Q/HFG
C
      IF(MODE.LE.0)THEN
         QU=Q
         GOTO 57
      END IF
C
C CALCULATION OF HEAT LOSSES FROM VAPOR LINE
C
      UL2=UL+UAV/((1-Z)*AC*FB)
C
C PRESSURE DROP DUE TO FRICTION IN VAPOR LINE
C
      VEL=XMR11/(pg*3600*VA)
      Re=ABS(Vel*Vd*pg/ng)
```

```
      FRICTN=1.0
      DO 73 I=1,10
         FRICTN=(1/(.87*ALOG(Re*SQRT(FRICTN))-.8))**2
73    CONTINUE
      delP=FRICTN/1000*VL*Vel**2*pg/(2*Vd)
      ZH=DELP/(PF*G)*1000
C
C SATURATION PRESSURE AND TEMPERATURE IN CONDENSER
C
      CALL Psat(Ref,T,Pt)
      Phx=Pt-delP
      IF(PHX.LE.0)THEN
         PHX=PIN
         THX=TI+.001
      ELSE
         TtK=T+273.3
         ThxK=1/(-R(ref)/hfg*alog(PHX/Pt)+1/TtK)
         Thx=ThxK-273.3
         dTv=Thx-T
      ENDIF
C
C PRESSURE DROP AND BOILING POINT ELEVATION
C             DUE TO HYDROSTATIC HEAD
C
      dP=pf*g*HEIGHT*(1-Z)*sin(B/180.*3.142)/1000.
      IF(DP.LT.0)DP=0
      Pb=Pt+dP
      TbK=1/(-R(ref)/hfg*alog(Pb/Pt)+1/TtK)
      Tb=TbK-273.3
      dTP=Tb-Thx
C
C SUBCOOLING DUE TO HEAT LOSSES FROM LIQUID LINE
C
      DTHL=UAL*(T-TA)/(XMR11*CPR11)
C
C TOTAL SUBCOOLING
C
      DTSC=DTP+DTHL
C
C AVERAGE TEMPERATURE IN BOILING SECTION
C
      TAVE=TB + (TB-T)/2
C
C CALCULATION OF Z
C
      if((TB-dTSC-Ta-S/UL)/(TB-Ta-S/UL).le.1)then
         z=0
      else
         z=XmR11*CpR11/(UL*Ac*Fl)
     *           *alog((TB-dTSC-Ta-S/UL)/(TB-Ta-S/UL))
```

```
      endif
      if(z.gt.1.0)z=1.0
C
C CALCULATION OF QUB, QUNB, & QU
C
      QB=AC*(1-Z)*FB*(S-UL2*(TAVE-TA))
      Qnb=XmR11*CpR11*dTP
      Q=Qnb+Qb
C
C SECANT METHOD FOR Z
C
      DUM=Z-Z0
      IF(ABS(DUM).GT..001)THEN
         IF(DUMNUM.EQ.1)THEN
            Z0=Z
            Z=.1
         ELSE
            DDUM=(DUM-DUM0)/DUM
            Z0=Z
            Z=Z0-DUM/DDUM
         ENDIF
         DUM0=DUM
         GOTO 55
      END IF
C
C SUBROUTINE HX CALCULATES THE UA FOR THE CONDENSER
C
      IF(MODE.EQ.2)THEN
      CALL HX(TI,XMC,XMR11,UA)
      ENDIF
C
C CALCULATION OF CONDENSER OUTLET TEMPERATURE AND QU
C
      Tcout=THX-(THX-Ti)*EXP(-UA/(xMc*Cp))
      QH=XMc*Cp*(Tcout-Ti)
C
C SECANT METHOD TO SOLVE FOR QU=QHX
C
      Y=Q-QH
      IF(ABS(Y)/Q.GT..001)THEN
         IF(NCOUNT.EQ.1)THEN
            T0=T
            T=T+5.0
         ELSE
            DT=T-T0
            if(abs(dT).le..01) goto 57
            DY=(Y-Y0)/DT
            T0=T
            T=T-Y/DY
         ENDIF
```

```
          Y0=Y
           if(t.le.0)t=0
           if(t.gt.150)t=150
          GOTO 50
       ENDIF
C
57     IF(XIT.GT.0)THEN
          EFFIC=Qu/(Ag*XIT)
          XX=(Ti-Ta)/XIT*3.6
       ELSE
          DFFIC=0
          XX=0
       END IF
       QU=Q
C
C OUTPUT
C
88     OUT(1)=Tcout
       OUT(2)=XMc
       OUT(3)=Ti
       OUT(4)=RHOD
       OUT(5)=XMR11
       OUT(6)=T
       OUT(7)=THX
       OUT(8)=DTSC
       OUT(9)=QU
       OUT(10)=XIT
       OUT(11)=XX
       OUT(12)=EFFIC
       OUT(13)=Z
       OUT(14)=TAUALF
C
       RETURN
       END
```

APPENDIX D

PROPERTY CALCULATION SUBROUTINES

This appendix contains the subroutines used to calculate the properties fo refrigerants. They only incluce data for R-11 and R-12.

Subroutine SATVAL calculates the heat of vaporization and the density, viscosity, conductivity and specific heats for both liquid and vapor phases. SATVAL is a quadratic interpolation of data from reference 24. Only saturation temperature (Tsat) and the type of refrigerant (r) need to be passed to SATVAL.

Subroutine PSAT calculates the saturation pressure of the refrigerant given the saturation temperature. Psat uses the equations of state developed by Martin in reference 27.

```
C ******************************************************
C                                                       *
C     DENSITY             p - kg/m3                     *
C     VISCOSITY           n - kg/m s                    *
C     CONDUCTIVITY        k - W/m C                     *
C     SPECIFIC HEAT       Cp - kJ/kg C                  *
C     ENTHALPY            hfg - kJ/kg                   *
C                                                       *
C     REFRIGERANTS        1 = R-11                      *
C                         2 = R-12                      *
C                                                       *
C ******************************************************
      SUBROUTINE SATVAL(Tsat,pf,pg,nf,ng,kf,kg,Cpf,
     *                  Cpg,hfg,r)
      REAL Ypf(3,2),Ypg(3,2),Ynf(3,2),Yng(3,2),Ykf(3,2),
     *     YCpf(3,2),Yhfg(3,2),XT(2),Ykg(3,2),YCpg(3,2)
     *    ,nf,ng,kf,kg,pf,pg,Cpf,Cpg,hfg
      Data Ypf/1518.2,1447.7,1371.1,1373.4,1266.4,1132.3/
     *     Ypg/3.23,8.84,20.,22.12,50.5,104.72/
      Data Ynf/.000504,.000377,.000297,.000252,.000199,
     *         .00016/
     *     Yng/.00001032,.00001137,.0000125,.000012,
     *         .0000136,.0000155/
      Data Ykf/.09265,.08425,.07591,.076,.065,.0539/
     *     Ykg/.0071,.0084,.0097,.0087,.0103,.01209/
      Data YCpf/.870,.897,.928,.942,1.0,1.16/
     *     YCpg/.565,.604,.655,.663,.77,.95/
      Data Yhfg/188.15,176.73,163.97,148.96,131.48,108.31/
      XT(1)=7.
      XT(2)=67.
      IF(TSAT.LT.XT(1))THEN
         T=XT(1)
      ELSE IF(TSAT.GT.XT(2))THEN
         T=XT(2)
      ELSE
         T=TSAT
      ENDIF
      CALL QVALUE(T,pf,XT,Ypf,r)
      CALL QVALUE(T,pg,XT,Ypg,r)
      CALL QVALUE(T,nf,XT,Ynf,r)
      CALL QVALUE(T,ng,XT,Yng,r)
      CALL QVALUE(T,kf,XT,Ykf,r)
      CALL QVALUE(T,kg,XT,Ykg,r)
      CALL QVALUE(T,Cpf,XT,YCpf,r)
      CALL QVALUE(T,Cpg,XT,YCpg,r)
      CALL QVALUE(T,hfg,XT,Yhfg,r)
      RETURN
      END
C ************************************
      SUBROUTINE QVALUE(XX,Y,XS,YS,ref)
```

```
      REAL LE,LE2,XS(2),YS(3,2),N(3)
      X=XX-XS(1)
      LE=XS(2)-XS(1)
      LE2=LE*LE
      X2=X*X
      N(1)=1-3*X/LE+2*X2/LE2
      N(2)=4*X/LE-4*X2/LE2
      N(3)=-X/LE+2*X2/LE2
      Y=0
      DO 5 I=1,3
         Y=Y+YS(I,ref)*N(I)
5     CONTINUE
      RETURN
      END
C  ***************************************************
C
C     SATURATION PRESSURE CALCULATION
C
C     TEMPERATURE INPUT IN C - CONVERTED TO R
C
C     PRESSURE CALCULATED IN psi - CONVERTED TO kPa
C
C
      SUBROUTINE Psat(r,T0,P0)
      REAL VP(6,2)
      DATA VP/42.14702865,-4344.343807,-12.84596753,
     *        0.004008372507,.0313605356,862.07,
     *        39.88381727,-3436.632228,-12.47152228
     *        ,.0047304244,0,0/
      T=(T0+273.3)*1.8
      IF(R.EQ.1.)THEN
         P=VP(1,r)+VP(2,r)/T+VP(3,r)*ALOG10(T)+VP(4,r)*T+
     *          VP(5,r)*(VP(6,r)-T)/T*ALOG10(VP(6,r)-T)
      ELSE IF(R.EQ.2.)THEN
         P=VP(1,r)+VP(2,r)/T+VP(3,r)*ALOG10(T)+VP(4,r)*T
      END IF
      P=10.0**P
      P0=P*6.8948
      END
```

```
C
C            CALCULATION OF THE
C      HEAT TRANSFER COEFFICIENT OF THE CONDENSER
C
       SUBROUTINE HX(Tc,XMc,XMR11,UAHX)
       COMMON FRACT,UA0
       IF(XMR11.LE.0)THEN
          UAHX=100
       ELSE
          L=26.
          Ai=3.8*FRACT
          Ao=10.6*FRACT
          ho=856*(L/(xmr11*2.2))**.33
          Tf=Tc*1.8+32
          Vfps=XMc*.00423
          hi=270*(1+.011*Tf)*Vfps**.8
          UAe=1/(1/(hi*Ai)+1/(ho*Ao))
          UAhx=UAe*1.9
       ENDIF
       IF(FRACT.EQ.99)UAHX=UA0
       RETURN
       END
```

References

1. McLaughlin, J.C., "Chairman's Corner: The Emergence of 'Second Generation' Solar Equipment," Solar Constant, SRCC News Letter, Vol. 11, No. 2, 4-5, May (1984).

2. ASHRAE 93-77, "Methods of Testing to Determine the Thermal Performance of Flat-Plate Solar Collectors,"ASHRAE, 1791, Tullie Circle, N.E., Atlanta, GA, 30329, revised printing (1978).

3. ASHRAE 109P, "Methods of Testing to Determine the Thermal Performance of Flat-Plate Solar Collectors Containing a Boiling Liquid," ASHRAE, 1791 Tullie Circle, N.E., Atlanta, GA, 30329 (1983).

4. Best, D., "What You Should Know about Phase-Change Water Heaters, Solar Age, 22-25, December (1981).

5. Sands, J., "Big Payoff for Phase-Change Heaters?," Solar Age, 38-44, November (1983).

6. Evans, R.D. and Greeley, D.N., "The Analysis, Design and Thermal Performance Testing of a Heat Pipe Flat-Plate Collector," 1977 Annual Meeting, Proceedings, American Solar Energy Society, Orlando, Florida, June 6-10 (1977).

7. Rush, C.K., "An Inherently Freeze Protected Solar Water Heater," 1983 Annual Meeting, Proceedings, American Solar Energy Society, Minneapolis, MN, June 1-3 (1983).

8. Soin, R.S., K.S. Rao, D.P.Rao and K.S. Rao, "Performance of Flat-Plate Solar Collectors with Fluids Undergoing Phase Change," Solar Energy, 23, p. 69 (1979).

9. Hottel, H.C. and Whillier, A., "Evaluation of Flat-Plate Collector Performance," Trans. of Conf. on Use of Solar Energy, Part 1, 74, University of Arizona Press (1958).

10. Schreyer, J.M., "Residentail Application of Refrigerant Charged Solar Collectors," Solar Energy, 26, 307-312 (1981).

11. Downing, R.C. and V.W. Waldin, "Phase-Change Heat Transfer in Solar Hot Water Heating Using R-11 and R-114," ASHRAE Trans. 86, Part I, 1980.

12. Fanney, A.H. and Terlizzi, C.P., "Testing of Refrigerants-Charged Solar Domestic Hot Water Systems," Building Equipment Division, Center for Building Technology, National Bureau of Standards, Washington, D.C., 20234, January (1984).

13. "Performance Evaluation of a Solar Heating and Cooling System Consisting of an Evacuated-Tube Heat Pipe Collector and Air Cooled Lithium Bromide Chiller," Final Report, Solar Energy Applications Laboratory Colorado State University, April (1984).

14. Al-Tamimi A.I., "Performance of Flat-PLate Solar Collector in a Closed-loop Thermosiphon Using Refrigerant-11," Ph.D. Thesis, Chemical Engineering Department, University of Michigan, Ann Arbor, September 1982.

15. Al-Tamimi, A.I. and Clark, J.A., "Thermal Analysis of a Solar Collector Containing a Boiling Fluid," 1983 Annual Meeting, Proceeding, American Solar Energy Society, Minneapolis, MN, June 1-3 (1983).

16. Al-Tamimi, A.I. and Clark, J.A., "Thermal Performance of a Solar Collector Containing a Boiling Fluid (R-11)," ASHRAE Winter Meeting Atlanta, GA, Jan 29 - Feb 2 (1984).

17. Abramzon, B., Yaron, I., and Borde, I., "An Analysis of a Flat-Plate Collector with Internal Boiling," ASME Transactions, Vol 105, 454-460, November (1983).

18. Klein, S.A., et al., "TRNSYS - A Transient Simulation Program," Engineering Experiment Station Report 38-12, University of Wisconsin-Madison (1983).

19. Mutch, J.J., "Residential Water Heating, Fuel Consumption Economics and Public Rotary, RAND, Dept. R1498, NSF (1974).

20. deWinter, F., "Heat Exchanger Penalties in Double-loop Solar Water Heating Systems," Solar Energy, 17, 335-337 (1975).

21. Duffie, J.A. and Beckman, W.A., Solar Engineering of Thermal Processes, Wiley Interscience, New York (1980).

22. Chapman, A.J., Heat Transfer, fourth edition, Macmillan Publishing Company, New York (1984).

23. Beckman, W.A., "Duct and Pipe losses in Solar Energy Systems," Solar Energy, 21, 531-532 (1978).

24. ASHRAE Handbook 1981 Fundamentals, ASHRAE, 1791 Tullie Circle, N.E., Atlanta, GA 30329 (1982).

25. Collier, J.G., Convective Boiling and Condensation, McGraw-Hill, (1972).

26. Van Wylen, G.J., and Sonntag, R.E., Fundamentals of Classical Thermodynamics, 2nd edition, revised printing, John Wiley & Sons, New York (1978).

27. Martin, J.J., "Correlations and Equations Used in Calculating Thermodynamic Properties of 'FREON' Refrigerants," Thermodynamic and Transport Properties of Gases, Liquids and Solids, p. 110, ASME, New York (1959).

28. "Thermodynamic Properties of FREON-11 Refrigerant," E.I. DuPont DeNemoors & Company, Wilmington, Delware 19898 (1965).

29. Wuestling, M.D., "Investigation of Promising Control Alternatives for Solar Water Heating Systems," M.S. Thesis, Mechanical Engineering Department, University of Wisconsin, Madison, December (1983).

30. McAdams, W.H., et al "Vaporization Inside Horizontal Tubes-II-Benzene-Oil Mixture," Trans, ASME, 64, 193 (1942).

31. Beckman, W.A., Klein, S.A. and Duffie, J.A., Solar Heating Design By the f-chart Method, Wiley-Interscience, New York (1977).